

PREPARATION OF ION-SELECTIVE MEMBRANE AND ELECTRODE USING COBALT
PORPHYRIN AS IONOPHORE FOR ANION DETECTION



A Thesis Submitted in Partial Fulfillment of the Requirements
for the Degree of Master of Science in Green Chemistry and Sustainability

Department of Chemistry

FACULTY OF SCIENCE

Chulalongkorn University

Academic Year 2022

Copyright of Chulalongkorn University

การเตรียมเมมเบรนเลือกจำเพาะไอออนและขั้วไฟฟ้าโดยใช้โพลีเมอร์ไฟรินเป็นไอออนฟอรัสำหรับ
การตรวจวัดไอออนลบ



วิทยานิพนธ์นี้เป็นส่วนหนึ่งของการศึกษาตามหลักสูตรปริญญาวิทยาศาสตรมหาบัณฑิต
สาขาวิชาเคมีสีเขียวและความยั่งยืน ภาควิชาเคมี
คณะวิทยาศาสตร์ จุฬาลงกรณ์มหาวิทยาลัย
ปีการศึกษา 2565
ลิขสิทธิ์ของจุฬาลงกรณ์มหาวิทยาลัย

Thesis Title	PREPARATION OF ION-SELECTIVE MEMBRANE AND ELECTRODE USING COBALT PORPHYRIN AS IONOPHORE FOR ANION DETECTION
By	Miss Kawisara Longsakpreecha
Field of Study	Green Chemistry and Sustainability
Thesis Advisor	Professor THAWATCHAI TUNTULANI, Ph.D.

Accepted by the FACULTY OF SCIENCE, Chulalongkorn University in Partial
Fulfillment of the Requirement for the Master of Science

..... Dean of the FACULTY OF SCIENCE
(Professor POLKIT SANGVANICH, Ph.D.)

THESIS COMMITTEE

..... Chairman
(Associate Professor FUANGFA UNOB, Ph.D.)

..... Thesis Advisor
(Professor THAWATCHAI TUNTULANI, Ph.D.)

..... External Examiner
(Associate Professor CHOMCHAI SUKSAI, Ph.D.)

จุฬาลงกรณ์มหาวิทยาลัย
CHULALONGKORN UNIVERSITY

6478028723 : MAJOR GREEN CHEMISTRY AND SUSTAINABILITY

KEYWORD: Potentiometry, Cobalt porphyrin, Ionophore, Perchlorate, Ion selective electrode

Kawisara Longsakpreecha : PREPARATION OF ION-SELECTIVE MEMBRANE AND ELECTRODE USING COBALT PORPHYRIN AS IONOPHORE FOR ANION DETECTION.

Advisor: Prof. THAWATCHAI TUNTULANI, Ph.D.

In this study, the synthesis of the 5,10,15,20-tetrakis(4-dodecyloxyphenyl)porphyrin cobalt(II) complex (CoL) was carried out through a condensation reaction of 4-n-dodecyloxybenzaldehyde and pyrrole, followed by the metalation reaction of cobalt(II) acetate with meso-tetra(4-alkyloxyphenyl) porphyrin (L_2) to obtain CoL. Characterization of CoL was conducted using physical methods such as $^1\text{H-NMR}$, $^{13}\text{C-NMR}$, and MALDI-TOF to confirm CoL structure and purity. CoL was utilized as an ionophore to fabricate the ion selective membrane (ISM) and ion selective electrode (ISE) for the detection of ClO_4^- . The composition of the ISM, including polymer (PVC), plasticizer (NPOE), cationic additive (TDMACl), and ionophore (CoL), was optimized for ISE fabrication. Various amounts of CoL and TDMACl were examined to determine the optimal conditions of the ISE. The optimized membrane components consisted of 33 wt% PVC, 66 wt% NPOE, 0.30 μmol CoL, and 60 mol% TDMACl compared to CoL. The fabricated ISEs exhibited a potentiometric response of -57.60 mV/decade ($R^2 = 0.99$) within a concentration range of 1×10^{-6} to 1×10^{-2} M for ClO_4^- detection. The detection limit was determined to be 2.13×10^{-6} M. Selectivity coefficient analysis using the separate solution method (SSM) demonstrated that ClO_4^- displayed the highest selectivity coefficient among other ions, with a detection limit of 2.13×10^{-6} M. The fabricated ISE demonstrated good reversibility and stability when measuring solutions within the pH range of 3 to 12. Furthermore, the fabricated ISEs were successfully applied to water samples, including different brands of drinking water, and exhibited satisfactory performance. Additionally, the fabricated ISEs showed promising characteristics for continuous monitoring and analysis of ClO_4^- in water samples.

Field of Study: Green Chemistry and
Sustainability

Student's Signature

Academic Year: 2022

Advisor's Signature

ACKNOWLEDGEMENTS

This thesis could not have been completed without the suggestions, inspiration, and encouragement of my thesis advisor, Prof. Thawatchai Tuntulani. Moreover, I would like to express my gratitude to Mr. Dumrongsak Aryuwananon and Prof. Buncha Pulpoka for providing CoL to initiate this work.

Additionally, I deeply appreciate the valuable discussions and suggestions from my thesis examination committee members, including Assoc. Prof. Fuangfa Unob and Assoc. Prof. Dr. Chomchai Suksai.

I would also like to acknowledge the financial support received from the scholarship provided by His Royal Highness Crown Prince Maha Vajiralongkorn Fund.

Furthermore, I would like to extend my gratitude to the Supramolecular Chemistry Research Unit (SCRU) and Environmental Analysis Research Unit (EARU) for providing the necessary research facilities.

Finally, I am immensely grateful to my family, friends, ZeeNunew, and others for their care, encouragement, and motivation throughout my graduate studies.



Kawisara Longsakpreecha

TABLE OF CONTENTS

	Page
.....	iii
ABSTRACT (THAI).....	iii
.....	iv
ABSTRACT (ENGLISH).....	iv
ACKNOWLEDGEMENTS.....	v
TABLE OF CONTENTS.....	vi
LIST OF TABLES.....	ix
LIST OF FIGURES.....	x
CHAPTER 1 INTRODUCTION.....	1
1.1 Background and significant of research.....	1
1.2 Theory and literature review.....	4
1.1.1 Perchlorate, properties, and toxicity.....	4
1.1.2 Ion selective electrode.....	5
1.1.3 Ionophore for anion selective electrode.....	8
1.3 Objectives and scope of the research.....	14
CHAPTER 2 EXPERIMENTAL SECTION.....	15
2.1 Materials.....	15
2.2 Synthesis and characterization of cobalt porphyrin.....	15
2.2.1 4-n-Dodecyloxybenzaldehyde.....	15
2.2.2 meso-tetra(4-alkyloxyphenyl) porphyrin.....	17
2.2.3 Meso-tetra(4-alkyloxyphenyl) porphyrin cobalt complex.....	18

2.3	Membrane preparation.....	19
2.4	Membrane optimization.....	19
2.5	Potentiometric measurement.....	20
2.6	Membrane selectivity.....	20
2.7	Membrane reversibility.....	21
2.8	Effects of the solution pH.....	22
2.9	Membrane reproducibility.....	22
2.10	Real sample analysis.....	22
2.11	Real-time analysis.....	23
CHAPTER 3	RESULTS AND DISCUSSION.....	24
3.1	Synthesis and characterization of cobalt porphyrin (CoL).....	24
3.2	Membrane preparation and optimization.....	26
3.2.1	Optimized amount of ionophore for enhanced performance.....	27
3.2.2	Optimization of amount of ionophore to the enhanced the performance of membrane.....	29
3.3	Membrane Performance.....	34
3.3.1	Membrane Selectivity.....	34
3.3.2	pH effect.....	37
3.3.3	Membrane reversibility.....	38
3.3.4	Membrane reproducibility.....	39
3.3.5	Real sample analysis.....	39
3.4	Real-time analysis.....	42
CHAPTER 4	CONCLUSION.....	44
REFERENCES	45

VITA..... 52



จุฬาลงกรณ์มหาวิทยาลัย
CHULALONGKORN UNIVERSITY

LIST OF TABLES

	Page
Table 3.1 Composition of membrane components and membrane appearance.....	28
Table 3.2 The difference amount of ionophore and potentiometric response toward different anions.	30
Table 3.3 The difference amount of TDMACl and potentiometric response toward different anions.....	32
Table 3.4 Selectivity coefficients of anions.....	35
Table 3.5 Calculation data of perchlorate selective electrode for real samples.....	41



LIST OF FIGURES

	Page
Figure 1.1 5,10,15,20-tetrakis(4-octyloxyphenyl) porphyrin cobalt (II) complex.....	2
Figure 1.2 5,10,15,20-tetrakis(4-dodecyloxyphenyl) porphyrins cobalt(II) complex (CoL).	3
Figure 1.3 Ion-selective electrode assembly with the working electrode, ion-selective membrane, and reference electrode. ⁴⁵	5
Figure 1.4 Potentiometric response of thiocyanate detection.....	6
Figure 1.5 chemical structure of common plasticizers.....	7
Figure 1.6 The chemical structure of Dodecabenzylbambus[6]uril (Bn12BU[6])......	9
Figure 1.7 Structure formulas of tetraphenyl porphyrin.	10
Figure 1.8 Structure formulas of porphyrin dimers used as ionophores.	11
Figure 1.9 Structure formulas of a) octaethyl porphyrin (TPP) and b) tetraphenyl porphyrin (OEP).....	12
Figure 1.10 Structure formulas of phosphorus(V) tetraphenylporphyrin complex.....	13
Figure 2.1 Experiment Setup for real-time analysis.....	23
Figure 3.1 Time trace line of ISE after adding ClO_4^- (1.0×10^{-7} to 1.0×10^{-2} M) to the solution.....	26
Figure 3.2 Calibration curve of average emf response for each analyte activity and $\log(a)$	27
Figure 3.3 Potentiometric response (emf) of anions with 0.3 μmol CoL and 20 mol% TDMACl.	30
Figure 3.4 Potentiometric response with difference amount of cationic additive toward SCN^-	32

Figure 3.5 Potentiometric response with difference amount of cationic additive toward ClO_4^-	33
Figure 3.6 Potentiometric response with difference amount of cationic additive toward NO_3^-	33
Figure 3.7 Potentiometric response (emf) of anions with 0.3 μmol CoL and 60 mol% TDMACL.	34
Figure 3.8 EMF response of the SCN^- and substituted with ClO_4^-	36
Figure 3.9 Potential response of the fabricated ISE with the difference pH a) 10^{-2} M of ClO_4^- and b) 10^{-3} M of ClO_4^-	37
Figure 3.10 Reversibility of ISE at the concentration between 1.0×10^{-3} and 1.0×10^{-2} M.	38
Figure 3.11 An example of Sing (drinking water) analysis.....	40
Figure 3.12 An example of Purra (drinking water) analysis.....	40
Figure 3.13 Experiment Setup for real-time analysis.....	42
Figure 3.14 The emf signal of two fabricated ISEs for real-time analysis.....	42

CHAPTER 1

INTRODUCTION

1.1 Background and significant of research

Anions are a significant source of environmental pollution commonly found in groundwater, surface water, and drinking water sources.¹⁻³ Anions such as perchlorate (ClO_4^-) and thiocyanate (SCN^-) can cause health hazards due to their inhibitory effects on thyroid hormone production, leading to disorders in iodide transportation to the thyroid gland.³⁻⁵

Various analytical methods, including ion chromatography, spectrophotometric techniques, complex formation with metal ions,^{6, 7} high-performance liquid chromatography with mass spectrometry,⁸ and gas chromatography,⁹ are employed to quantify anion concentrations. While these methods offer advantages, they also suffer from disadvantages such as the need for complex instrumentation, high costs, and time-consuming procedures.

Therefore, this study aims to address these limitations by focusing on the development of ion selective electrodes (ISEs) as sensors for anion detection. ISEs offer the advantages of low operational costs and reduced time requirements. A crucial component of ISEs is the ion-permeable membrane, which exhibits selectivity toward specific ions. Typically, ISE membranes are lipophilic, immiscible with water, and composed of a polymer, plasticizer, ionic additive, and ionophore.¹⁰ The selectivity and sensitivity of the ISE membrane in measuring specific anions depend on the proportions of the plasticizer, ionophore, and ionic additive.¹¹⁻¹³ Selective ionophores are lipophilic complexing agents that can reversibly bind ions and may exist in electrically neutral or charged forms. In the context of anion detection, ionophores must possess coordination sites to facilitate the transport of anions into

the membrane phase.¹⁴ Metal complex ionophores have been extensively used in anion selective electrodes.¹⁵⁻²⁰ However, our focus will be on metal porphyrin complexes as ionophores. Porphyrins have been widely employed as ionophores in ion sensors for both anions and cations due to their favorable properties, such as excellent selectivity, sensitivity, and low toxicity. The selectivity of metal-porphyrins, which vary in metal center and substituents on the porphyrin structure, can be tailored to target specific ions. Additionally, the incorporation of ionic additives in the membrane matrix is necessary to enhance ion exchanger kinetics, ionic mobility, and reduce membrane resistance.

In 2021, our research group employed a 5,10,15,20-tetrakis(4-octyloxyphenyl) porphyrin cobalt (II) complex, as illustrated in **Figure 1.1**, as an ionophore within a portable paper-based optode for the quantification of thiocyanate in urine samples. The developed optode exhibited remarkable sensitivity and selectivity towards thiocyanate compared to other anions. This finding was reported in previous study.²¹

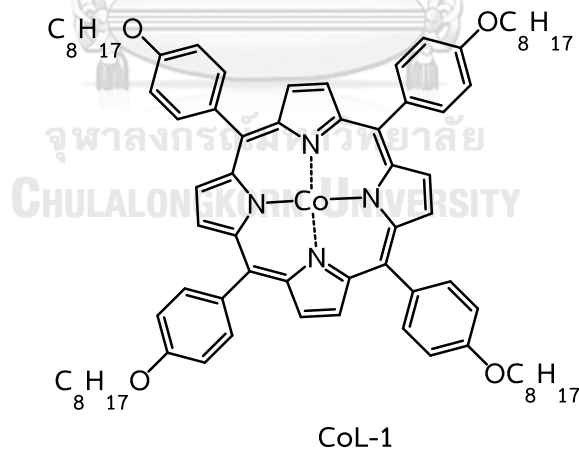


Figure 1.1 5,10,15,20-tetrakis(4-octyloxyphenyl) porphyrin cobalt (II) complex (CoL-1).²¹

Our research group is particularly interested in developing ion selective electrodes for anion detection, with a specific focus on utilizing the 5,10,15,20-

tetrakis(4-dodecyloxyphenyl) porphyrins cobalt(II) complex (CoL) as an ionophore. CoL, depicted in **Figure 1.2** is similar to CoL-1 and selected as the ionophore due to its remarkable coordinating properties, enabling anion coordination at the axial position. The porphyrin unit of CoL possesses longer chain hydrocarbon substituents compared to CoL-1, resulting in improved solubility within the membrane.^{14, 22} This characteristic ensures a homogeneous mixture with all membrane components¹⁶ and prevents leakage of the ionophore into the aqueous phase. Additionally, the planar structure and longer chain hydrocarbon substituents contribute to the ionophore's increased hydrophobicity, enhancing its ability to efficiently transport ions within the membrane phase. The primary objective of this thesis is to fabricate ion-selective electrodes (ISEs) by adjusting the ratios of all membrane components, including the ionophore, plasticizer, and ionic additive, to achieve the desired characteristics necessary for detecting specific anions.²³ Subsequently, the fabricated ISEs will undergo further investigation to evaluate their potential for real-time monitoring of specific anions in real samples.

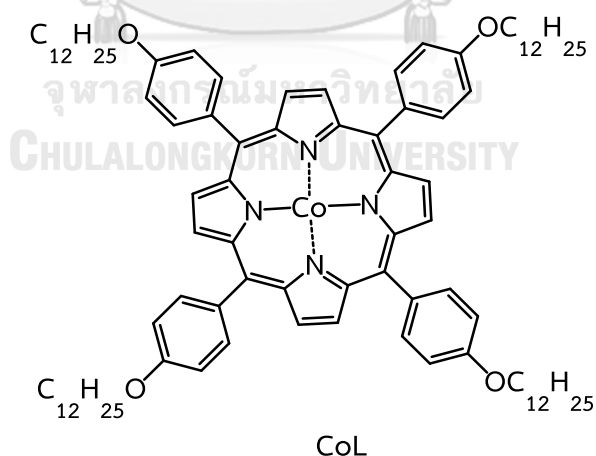


Figure 1.2 5,10,15,20-tetrakis(4-dodecyloxyphenyl) porphyrins cobalt(II) complex (CoL).

1.2 Theory and literature review

1.1.1 Perchlorate, properties, and toxicity

Perchlorate, a highly reactive chemical compound composed of chlorine and oxygen, has raised significant concerns due to its potential presence and toxicity in water sources.²⁴⁻²⁶ It is commonly used in various industrial processes, such as the manufacturing of explosives, rocket propellants, and fireworks.²⁷⁻²⁹ Additionally, perchlorate can be found in fertilizers and has been utilized in the production of airbag inflators in automobiles.^{30, 31} The widespread use and solubility of perchlorate contribute to its potential for contamination in water systems, particularly groundwater.^{32, 33} Its persistence in the environment has raised alarms about its detrimental effects on ecosystems and human health. Studies have indicated that perchlorate can interfere with the proper functioning of the thyroid gland by inhibiting the uptake of iodine, a crucial element required for thyroid hormone synthesis. Consequently, prolonged exposure to perchlorate has been associated with thyroid dysfunction, including hypothyroidism. Vulnerable populations, such as pregnant women, infants, and individuals with pre-existing thyroid conditions, are particularly at risk.³⁴⁻³⁶ The presence of perchlorate in water sources necessitates effective monitoring and detection methods to safeguard public health and ensure the quality of drinking water. Various analytical methods, including ion chromatography,^{37, 38} spectrophotometric methods,⁶ high-performance liquid chromatography with mass spectrometry,⁸ and stripping cyclic voltammetry³⁹ are commonly employed to quantify the concentration of anions. However, these methods suffer from several drawbacks, such as the requirement of complex instruments, high costs, and time-intensive procedures. The aim of this study is to investigate an alternative technique that can overcome these limitations by developing an ion selective electrode. Many studies have utilized ion selective

electrodes for perchlorate detection.⁴⁰⁻⁴⁴ This approach offers several advantages, including cost-effectiveness, time-efficiency, and the ability to provide rapid results.

1.1.2 Ion selective electrode

Ion-selective electrode (ISEs) is an analytical instrument. ISEs have an application as well-established routine analysis techniques in many fields such as clinical and environmental analysis, physiology, and process control. ISEs consist of the reference electrode, indicator electrode, and potentiometer that is placed between them as shown in **Figure 1.3**. The reference electrode gives the stable potential to measure the potential of indicator electrode against. The potentiometer is used to measure the potential difference between the reference and indicator electrode.

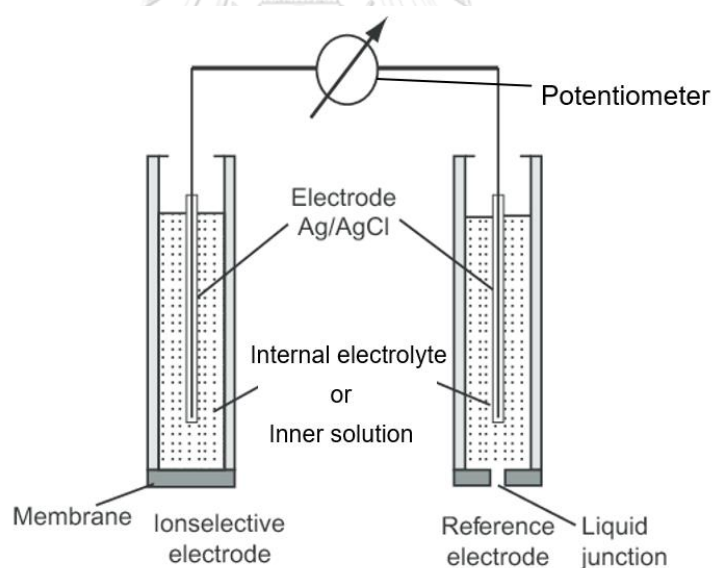


Figure 1.3 Ion-selective electrode assembly with the working electrode, ion-selective membrane, and reference electrode.⁴⁵

At the equilibrium, the potential difference between two existing sides of the membrane was measured and can be described by the Donnan potential as shown in Eq 1.1.

$$E_M = E^0 + 2.303 \frac{RT}{zF} \ln (a_1(\text{aqueous})/a_2(\text{organic})) \quad (1.1)$$

Where E_M is the membrane potential, E^0 is a constant characteristic of a particular ISE, R is a gas constant (8.314 J/K·mol), F is the Faraday's constant (96,485 C/mol), T is the temperature (in K), z is the charge of the analyte ion, and $a_1(\text{aqueous})$ and $a_2(\text{organic})$ are the activity of the measured ion in aqueous and organic phase, respectively.⁴⁶

For the anion detection, a particular potentiometric response is shown in Figure 1.4. The potential difference will decrease when the concentration of anion in the analyte increases due to the negative z value which can be described by Eq 1.1.

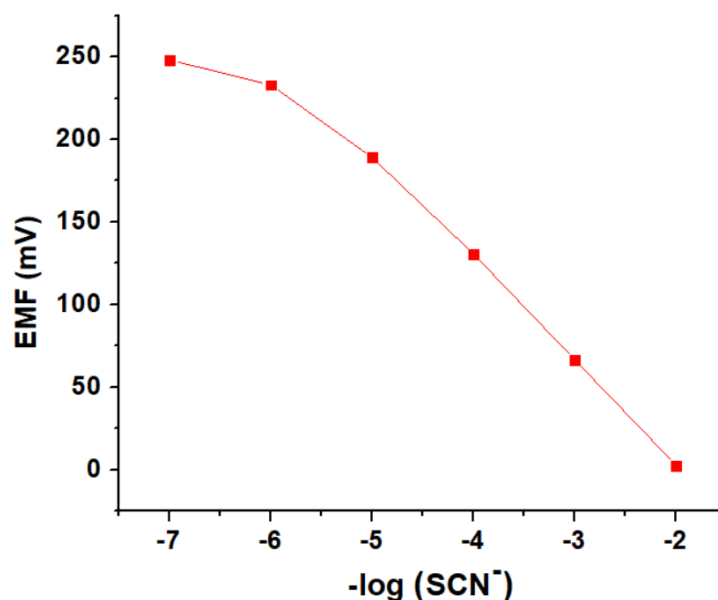


Figure 1.4 Potentiometric response of thiocyanate detection.

The composition of ion-selective membranes includes a polymer such as PVC, a plasticizer such as NPOE, an ionic additive (cationic additive for anions detection) such as TDMACl, and ionophore such as CoL. Plasticizers must have the following properties such as reducing transition glass, solubilizing the ionophore, insoluble in water, and inert with ion additive. These plasticizers contribute to the passage of ions through the membrane and possess selective properties towards specific ions. The polarity of each plasticizer induces the aggregation of ionophores, resulting in the mobility of ion carriers.^{11, 12} The structure of common plasticizers is shown in **Figure 1.5**.

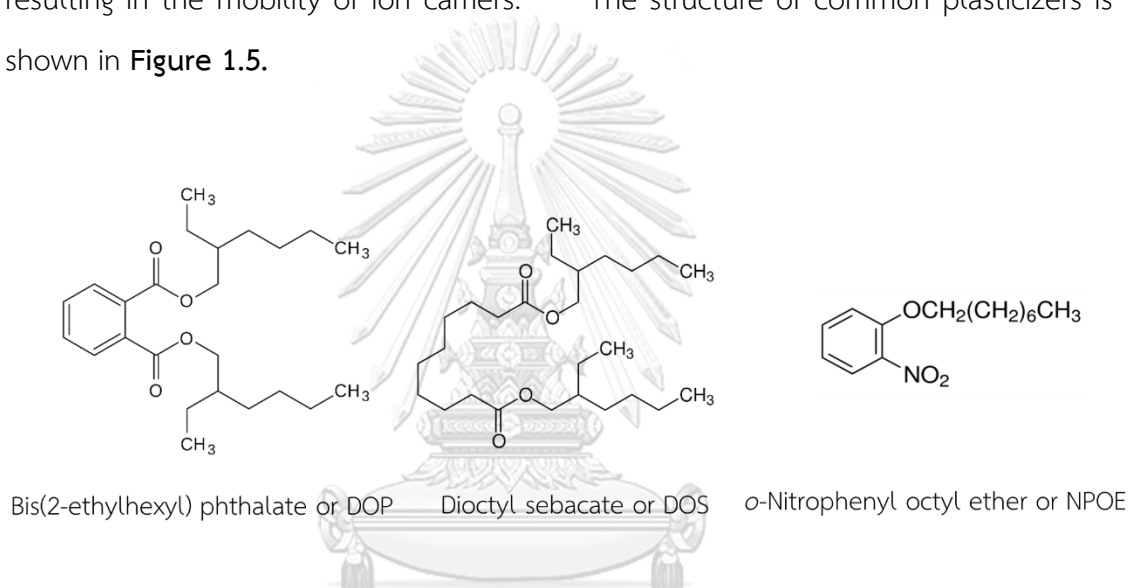


Figure 1.5 chemical structure of common plasticizers.

Dana et al.⁴⁷ conducted research on the detection of iodide and bromide ions in the medically monitored concentration range. NPOE and DOP were employed as plasticizers for iodide and bromide detection, respectively. The membrane containing NPOE as a plasticizer exhibited selectivity towards I^- . The authors proposed that NPOE aided in dispersing the ionophore within the membrane phase by forming coordination bonds with larger anions. In this study, we report the use of NPOE as a plasticizer, which exhibits a polar structure compared to other plasticizers. This characteristic makes NPOE suitable for our ionophore (CoL), which possesses a non-polar structure.

The selectivity of a polymeric membrane is a crucial characteristic for potentiometric sensors. It refers to the reliability of measuring the analyte of interest. Theoretical selectivity encompasses key parameters that contribute to the performance of potentiometric electrodes, such as adjusted weighting parameters (e.g., absolute membrane concentrations) or the choice of different plasticizers. The determination of selectivity coefficients can be achieved using Nernst's equation (**Eq 1.1**) through two different measuring methods known as the Nicolskii-Eisenman formalism (**Eq 1.2**). These methods include the Separate Solution Method (SSM) and the Fixed Interference Method (FIM). SSM involves measuring two separate solutions, each containing only the specific ion of interest.

$$K_{i,j}^{\text{pot}} = \frac{a_i}{z_i/z_j} \exp \frac{E_i E_j}{RT} Z_i F \quad (1.2)$$

In this study, the Nicolskii selectivity coefficient is calculated using the SSM approach and is derived from two observed potentials (**Eq 1.2**).^{11, 48} E_i represents the potential response of the primary ion, E_j represents the potential response of the interfering ion, a_i is the activity of the primary ion in the solution without interfering ions, a_j represents the activities of the primary and interfering ions, respectively. Z_i and Z_j represent the charges of the primary and interfering ions, and $K_{i,j}^{\text{pot}}$ is the selectivity coefficient.

1.1.3 Ionophore for anion selective electrode

Ionophores or ion carriers are essential components in membrane electrodes, fulfilling the role of complexing agents. These compounds, characterized by macrocyclic structures and transition metal complexes, exhibit potential selectivity towards specific ions. The response of the membrane's electromotive force (emf) is

believed to arise from the binding of these complexes to the axial position of the metal center. Several metal complexes with diverse ligands including cobaloxime, phthalocyanine, salens, pyrrole, uranil, dioxaoctane and tetraphenyl porphyrin have been documented as effective ionophores for perchlorate⁴⁹ and other anions.⁵⁰⁻⁵²

Petra et al.⁵³ conducted a study where they employed dodecabenzylbambus[6]uril (Bn12BU[6]), depicted in **Figure 1.6**, as an ionophore for creating a specialized membrane in solid contact ion selective electrodes. The reason for using Bn12BU[6] is its strong binding ability with perchlorate ions, thanks to the favorable match in size between the ion and the receptor cavity. The ion selective electrodes (ISEs) demonstrated a fast response and exhibited a sub-Nernstian slope of approximately 57.0 mV/decade during potentiometric measurements of perchlorate solutions. These measurements were taken within the concentration range of 10^{-1} to 10^{-6} M. Additionally, the ISEs displayed high stability and adequate selectivity towards other common inorganic anions like bromide, chloride, nitrate, and sulfate.

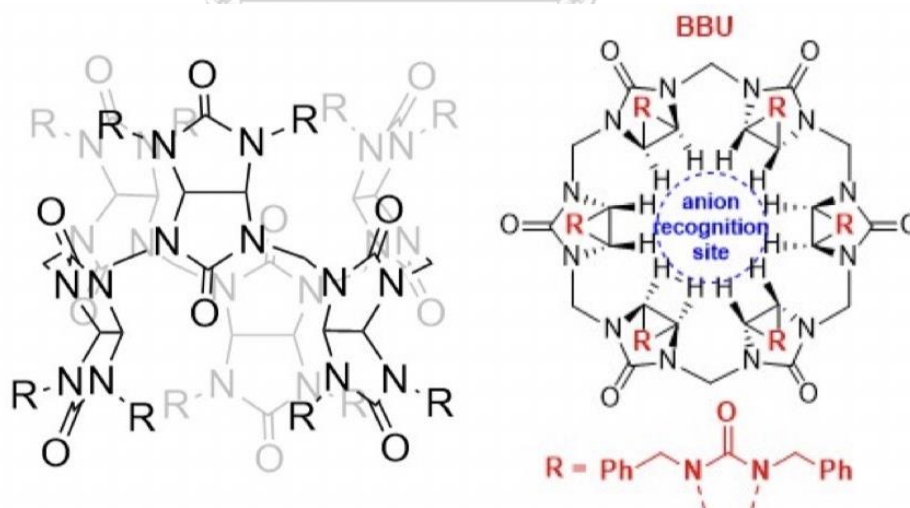


Figure 1.6 The chemical structure of Dodecabenzylbambus[6]uril (Bn12BU[6]).

Chen et al.⁵⁴ focused on the detection of CN^- in drinking water while overcoming interference from OH^- . Zn(II) tetraphenyl porphyrin, showed in **Figure 1.7**, was chosen as the ionophore due to its suitable coordination with CN^- , enabling CN^- to coordinate with the axial ligand and the central metal (Zn). The researchers achieved significant improvement in the selectivity of the membrane for CN^- detection and obtained the highest selectivity and sensitivity for CN^- ion-selective membranes. The determined concentration of CN^- was found to be lower than the maximum permissible concentration in drinking water in the U.S.A. This study demonstrates the successful utilization of Zn(II) tetraphenyl porphyrin as an effective ionophore for selective CN^- detection.

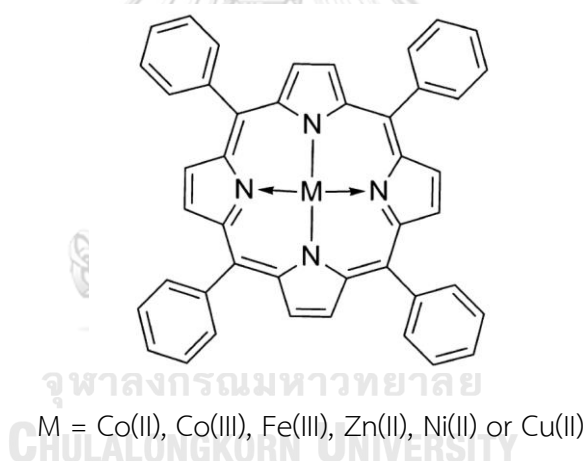


Figure 1.7 Structure formulas of tetraphenyl porphyrin.

Grzegorz et al.⁵⁵ conducted a study in which they investigated the use of four different porphyrin dimers, as shown in the **Figure 1.8**. These dimers were employed in the field of electroanalysis, specifically for the potentiometric determination of ions. The dimers consisted of porphyrin units that were sensitive to anions and were integrated into sensors designed to detect anions. These dimers exhibited sensitivity

towards various types of anions. Notably, the sensors utilizing these anion-sensitive dimers demonstrated selectivity towards ClO_4^- . The selectivity of the sensors primarily depended on the specific porphyrin dimers utilized in the ion-selective membrane. Furthermore, the study suggests that dimerizing single porphyrins has the potential to enhance or modify the selectivity of porphyrins in detecting ions.

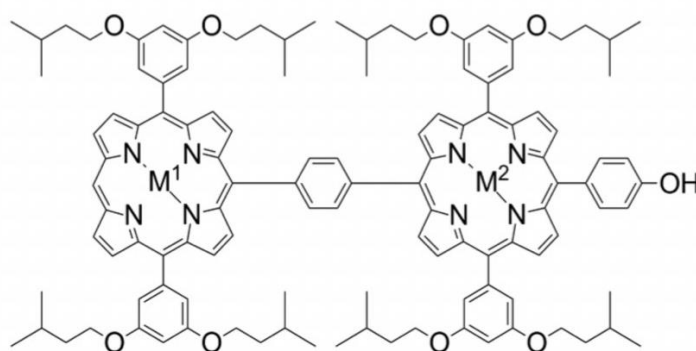


Figure 1.8 Structure formulas of porphyrin dimers used as ionophores.

Mitchell-Koch et al.⁵⁶ investigated the use of aluminum(III) porphyrins as ionophores in polymeric membranes for the detection of fluoride (F^-). They utilized octaethyl porphyrin (TEPP), as illustrated structure in **Figure 1.9 a**), and tetraphenyl porphyrin (OEP), as illustrated structure in **Figure 1.9 b**), to form complexes with Al(III) as ionophores selective for F^- , specifically avoiding lipophilic anions like perchlorate and thiocyanate. The researchers observed that the steric hindrance provided by the OEP porphyrin prevented bridging between fluoride and the metal center, resulting in improved ionophore performance. The optimized membrane achieved a limit of detection as low as $40 \mu\text{M}$ for fluoride ions. This study highlights the successful application of aluminum (III) porphyrins as selective ionophores for the detection of F^- .

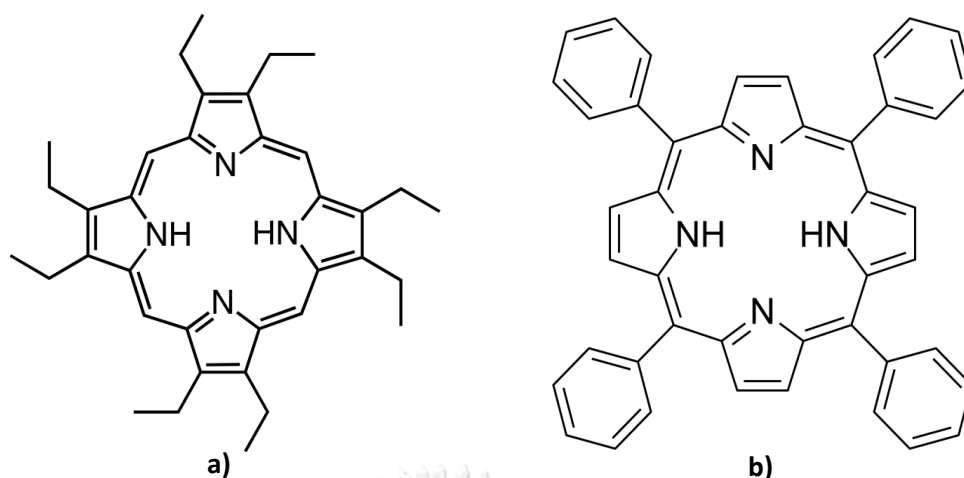


Figure 1.9 Structure formulas of a) octaethyl porphyrin (TPP) and b) tetraphenyl porphyrin (OEP)

Mojtaba et al.⁵⁷ conducted a study to develop perchlorate-selective electrodes using a phosphorus(V) tetraphenylporphyrin complex, as depicted in **Figure 1.10**. The electrodes demonstrated near-Nernstian responses across a wide concentration range of ClO_4^- ions, ranging from 8.0×10^{-6} to 1.6×10^{-1} M for the polymeric membrane (PME) and from 1.0×10^{-6} to 3.0×10^{-2} M for the coated glassy carbon (CGCE). Notably, they exhibited low detection limits, with the PME achieving a detection limit of 5.0×10^{-6} M and the CGCE achieving a detection limit of 7.0×10^{-7} M. These electrodes exhibited favorable characteristics such as low resistance, fast response times, and long lifetimes. Importantly, they also demonstrated high selectivity compared to other common anions.

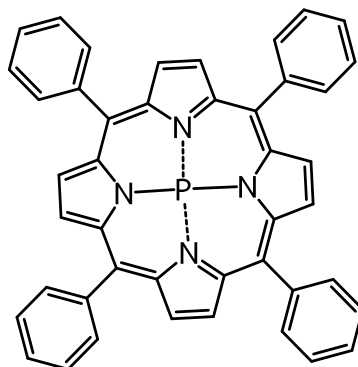


Figure 1.10 Structure formulas of phosphorus(V) tetraphenylporphyrin complex.

The ion-selective electrode (ISE) is a valuable tool for real-time analysis, enabling accurate monitoring of specific ions in various solutions. Its selective response, combined with additional components like valves, pumps, and ionophores, enhances sensitivity and selectivity. Han et al.⁵⁸ utilized an ion-selective electrode to conduct continuous monitoring of the concentration of macronutrients, namely NO_3^- , K^+ , and Ca^{2+} , in hydroponic solutions. Their real-time analysis system was comprised of a valve and pumps, which facilitated the collection of samples for measurement purposes. For the fabrication of the membrane, Ca ionophore II was employed as the ionophore, allowing for effective sensing of NO_3^- , K^+ , and Ca^{2+} in hydroponic environments. Importantly, this membrane exhibited a strong linear correlation ($R^2 > 0.84$) with the macronutrient concentrations under investigation.

Based on the available literature, porphyrins have demonstrated their effectiveness as ionophores in ion sensors for both anions and cations. These compounds possess favorable attributes, including notable selectivity and sensitivity, along with a low toxicity profile. The selectivity of these ion sensors can be modulated by utilizing metal-porphyrin complexes featuring diverse metals and porphyrin structures, thereby influencing the charge and configuration of the complexes. To optimize the performance of the electrode, the inclusion of an ionic additive within the matrix becomes essential. This additive plays a pivotal role in

augmenting ion exchanger kinetics and facilitating enhanced ionic mobility within the electrode matrix, consequently reducing electrode resistance.

1.3 Objectives and scope of the research

The objective of this study is to prepare and optimize ion-selective membranes (ISMs) and ion-selective electrodes (ISEs) for the detection of anions, specifically using CoL as the ionophore. The optimization process involves adjusting the ratio of components in the membrane, including the ionophore (CoL) and the cationic additive (TDMACl). Subsequently, the sensitivity, selectivity, reversibility, limit of detection, effect of pH and reproducibility of the fabricated ISEs will be investigated under the optimized conditions. The ultimate goal is to use the fabricated ISEs in analysis of ClO_4^- in real samples and explore a potential application in real-time analysis.

CHAPTER 2

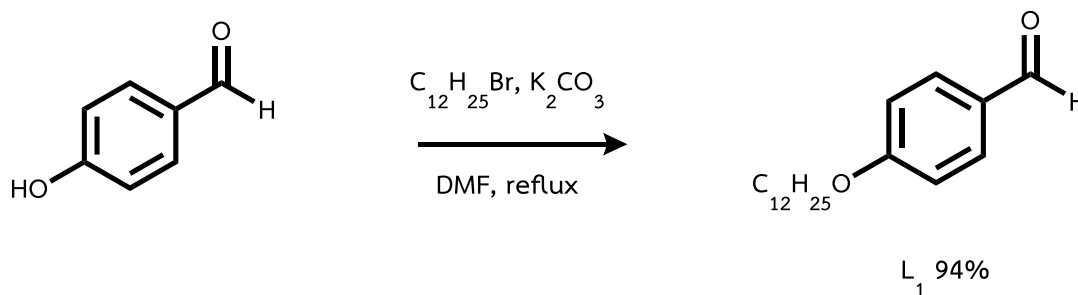
EXPERIMENTAL SECTION

2.1 Materials

Tridodecylmethylammonium chloride (TDMACl), polyvinylchloride (PVC), high molecular weight polyvinyl chloride, 1-(2-nitrophenoxy) octane (NPOE), tetrahydrofuran (THF) were obtained from Fluka with Selectophore® grade. Aqueous solutions were prepared with ultrapure water from Milli-Q (Bedford, MA, USA) water purification system (Millipore). Pyrrole and 4-n-dodecyl-loxybenzaldehyde were purchased from TCL Japan. Propionic acid, toluene, methanol, and N,N-dimethylformamide (DMF) were purchased from Merck (Darmstadt, Germany) and used without further purification. Hexane and dichloromethane were purchased from Merck (Darmstadt, Germany). Cobalt (II) acetate was purchased from BDH Chemical Ltd (Poole, UK).

2.2 Synthesis and characterization of cobalt porphyrin

2.2.1 4-n-Dodecyloxybenzaldehyde



Scheme 2.1 The synthesis of 4-n-dodecyloxybenzaldehyde (L_1).

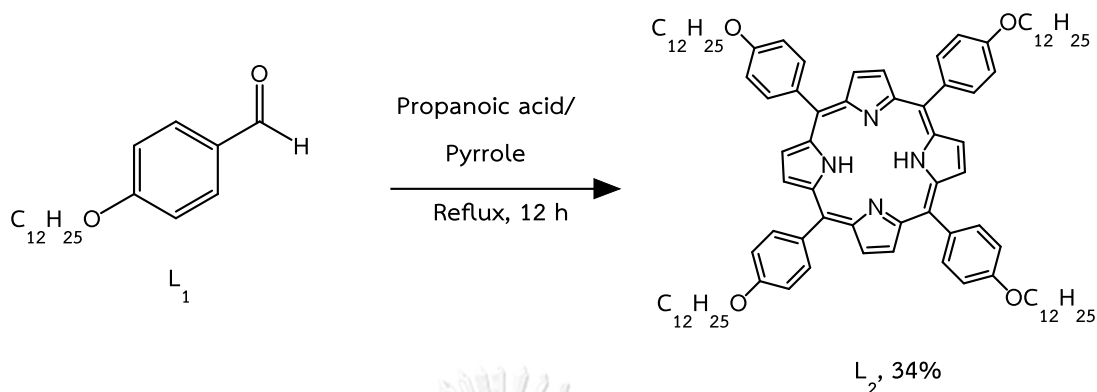
In the experimental procedure, a mixture of 4-Hydroxybenzaldehyde (4.00 g, 32.8 mmol) and anhydrous potassium carbonate (5.00 g, 36.2 mmol) was dissolved in 25.0 mL of dry N,N-dimethylformamide. The resulting solution was subjected to stirring and heated to reflux following the procedure depicted in **Scheme 2.1**. Subsequently, 1-Bromododecane (9.00 g, 36.2 mmol) was introduced into the mixture, and the heating process was sustained until the reaction reached completion. Afterward, the reaction mixture was dissolved in water and subjected to extraction with ethyl acetate in three sequential steps. The organic layer obtained from each extraction was then subjected to washing with water and drying using anhydrous sodium sulfate. The solvents were subsequently removed under *vacuo*. The resulting product was subjected to purification using silica gel column chromatography. This purification method yielded a colorless oil weighing 8.93 g (equivalent to a 94% yield) with an R_f value of 0.36 (Hexane: Ethyl Acetate, 19:1).

Characteristic data for L₁: ¹H-NMR spectrum (500 MHz, CDCl₃, δ (ppm)): 9.78 (s, 1H, CHO), 7.73 (d, J = 8.8 Hz, 2H), 6.90 (d, J = 8.7 Hz, 2H), 3.94 (t, J = 6.6 Hz, 2H), 1.75-1.69 (m, 2H), 1.41-1.18 (m, 18H), 0.80 (t, J = 7.0 Hz, 3H).

Characteristic data for L₁: ¹³C-NMR spectrum (125 MHz, CDCl₃, δ (ppm)): 190.75, 164.32, 132.00, 129.81, 114.78, 68.46, 31.99, 29.73, 29.71, 29.66, 29.63, 29.42, 29.12, 26.03, 25.88, 22.76, 14.18.

MALDI-TOF MS calculated. for C₁₉H₃₀O₂ = 290.22 m/z, found = 290.435 m/z.

2.2.2 meso-tetra(4-alkyloxyphenyl) porphyrin



Scheme 2.2 The synthesis of meso-tetra(4-alkyloxyphenyl) porphyrin (L_2).

A quantity of 4-n-Dodecyloxybenzaldehyde (1.00 g, 3.44 mmol) was dissolved in propionic acid. The resulting solution was heated to reflux with continuous stirring for a duration of 30 minutes. Subsequently, Pyrrole (0.230 g, 3.44 mmol) was slowly added to the heated solution, and the heating process was continued until the reaction reached completion, as depicted in **Scheme 2.2**. Following completion of the reaction, the mixture was cooled to room temperature, and methanol was introduced into the reaction mixture. The resulting product was then filtered and washed with methanol, resulting in the formation of a dark-purple solid. The crude product underwent purification through column chromatography and subsequent recrystallization, leading to the production of purple crystals weighing 0.394 g (34% yield). The product exhibited an R_f value of 0.30 (Hexane: DCM, 8:2 ratio).

Characteristic data for L_1 : $^1\text{H-NMR}$ spectrum (500 MHz, CDCl_3 , δ (ppm)): 8.87 (s, 8H, β -H), 8.10 (d, $J = 8.4$ Hz, 8H), 7.26 (d, $J = 8.5$ Hz, 8H), 4.23 (t, $J = 6.5$ Hz, 8H), 2.00-1.94 (m, 8H), 1.62-1.32 (m, 72H), 0.91 (t, $J = 6.9$ Hz, 12H), -2.73 (s, 2H).

Characteristic data for L_1 : $^{13}\text{C-NMR}$ spectrum (125 MHz, CDCl_3 , δ (ppm)): 159.04, 135.69, 134.53, 119.91, 112.78, 68.41, 32.06, 29.83, 29.78, 29.64, 29.61, 29.50, 26.34, 22.82, 14.25.

MALDI-TOF MS calculated. for $C_{92}H_{126}N_4O_4$ = 1350.98 m/z, found = 1350.679 m/z.

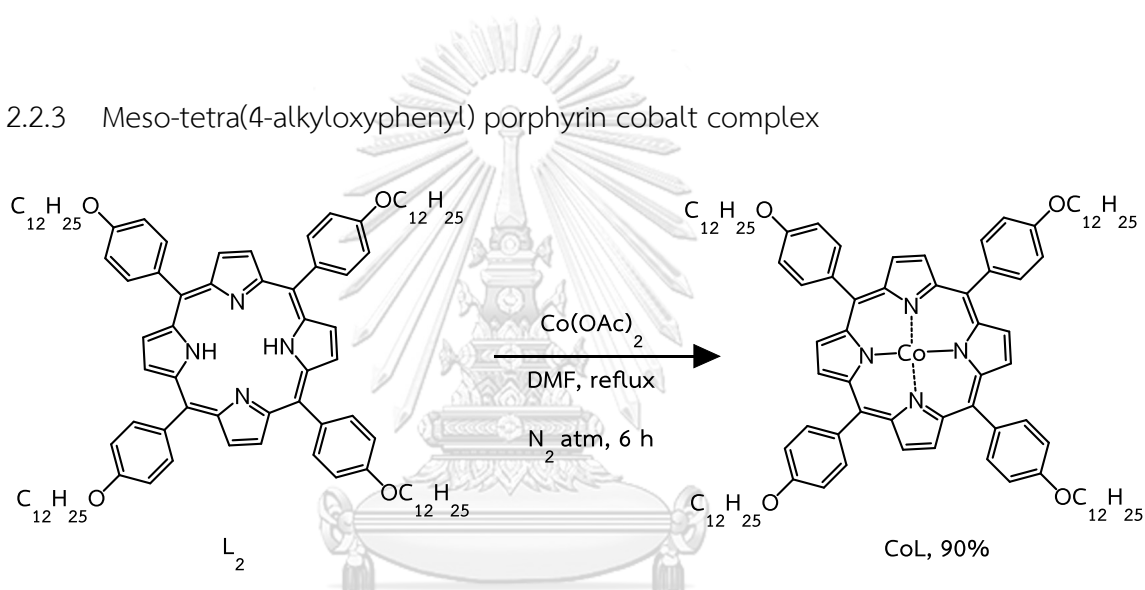
Elemental analysis: Anal calcd. for $C_{92}H_{126}N_4O_4$: C, 81.73; H, 9.39; N, 4.14.

Found: C, C, 81.63; H, 9.41; N, 4.21.

FT-IR, ν_{\max} (cm^{-1}): 3314.47, 2918.72, 2848.86, 1604.46, 1507.01, 1463.23, 1239.43, 1172.88, 965.66, 840.35, 801.69, 789.32, 738.52.

UV-vis, λ_{\max} (nm): 423, 520, 557, 596, 652.

2.2.3 Meso-tetra(4-alkyloxyphenyl) porphyrin cobalt complex



Scheme 2.3 The synthesis of meso-tetra(4-alkyloxyphenyl) porphyrin cobalt complex (CoL)

The porphyrin compound (L_2) (1.35 g, 1.00 mmol) was dissolved in 20.0 mL of dry dimethylformamide (DMF) and subjected to heating under a nitrogen atmosphere. Cobalt acetate (0.885 g, 5.00 mmol) was dissolved in 5.00 mL of dry DMF and added to the L_2 solution, following the procedure outlined in **Scheme 2.3**. The resulting mixture was stirred under reflux until the reaction reached completion, as confirmed by TLC analysis (6 h). Subsequently, the reaction mixture was dissolved in water and subjected to extraction with dichloromethane. The organic layer obtained from the extraction was washed twice with water, dried using anhydrous

sodium sulfate, and concentrated under vacuum. The crude product underwent purification through column chromatography on silica gel and recrystallization using a mixture of dichloromethane and methanol. This purification process yielded the desired porphyrin metal complex CoL, weighing 1.27 g (90% yield).

MALDI-TOF MS calculated. for $C_{92}H_{124}CoN_4O_4 = 1407.90$ m/z, found = 1407.935 m/z.

UV-vis, λ_{max} (nm): 416, 531.

2.3 Membrane preparation

Cocktail solution is prepared by mixing PVC 72.6 mg, NPOE 145.2 mg, porphyrins cobalt complex (0.100, 0.200, and 0.300 μmol), and TDMACI (20.0, 40.0, 60.0 mol% compared to ionophore) in a vial. Then THF (2.00 mL) was added to the mixture and the solution was stirred for 3 mins. After completion, solutions were gradually poured on a glass slide and left in the fume hood at room temperature overnight to allow slow evaporation of the solvent. Then, the membrane was cut into small sizes and conditioned with 0.0100 M solutions of each anion overnight before use as an anion selective membrane in ISEs.

2.4 Membrane optimization

The membrane was optimized by varying the ratios of the ionophore (CoL) in three different quantities: 0.100 μmol , 0.200 μmol , and 0.300 μmol , along with the cationic additive (TDMACI) in three different proportions: 20.0 mol%, 40.0 mol%, and 60.0 mol%, all relative to the ionophore. Initially, the quantity of ionophore was varied while keeping the amount of cationic additive fixed at 20 mol% relative to the

ionophore, as well as maintaining the other components, PVC and NPOE, constant. This was done to determine the optimal ISE. Subsequently, the amount of cationic additive was varied while maintaining the quantity of ionophore at 0.3 μmol and keeping the other components unchanged.

2.5 Potentiometric measurement

The potential measurements were carried out at $25.0 \pm ^\circ\text{C}$ using EMF 16 Precision Electrochemistry EMF Interface connecting with L-EMF Data Acquisition System (L-EMF DAQ) program, Lawson Lab, Inc. The following assembly was set up: Ag/AgCl | internal solution ($\text{ClO}_4^- 1.00 \times 10^{-2} \text{ M} + \text{Cl}^- 1.00 \times 10^{-3} \text{ M}$) | membrane electrode | test solution.

The potential analysis of any solution was recorded when it became stable after adding standard concentration of each ion. The plots between logarithmic function of anion concentration and average potential may be used to calculate a Nernstian response slope and limit of detection (LOD). The activities of anions were based on the activity coefficient (γ) which calculated from Debye-Hückel equation.

2.6 Membrane selectivity

The selectivity of the membrane was studied by using the Separate Solution Method (SSM). The potentiometric selectivity coefficients are calculated by following the Eq 2.1.

$$\log K_{a_i, j}^{\text{Pot}} = \frac{nF(E_j - E_i)}{2.303RT} + \log \left(\frac{a_i}{a_j^{n/m}} \right) \quad (2.1)$$

Where $\log K_{a_i, j}^{\text{Pot}}$ is the potentiometric selectivity coefficient, n and m = charges of primary and interfering ions, respectively. E_i is the measured cell potential at primary ion activity a_i and E_j is the measured cell potential at interfering ion activity a_j , R , T , and F are gas constant, temperature, and faradaic constant, respectively.

The fabricated membranes were conditioned by soaking them in a solution containing interfering anions at a concentration of 1.0×10^{-2} M. Initially, the electrode's response was assessed by measuring its reaction to identical interfering metal ions, ranging from 10^{-7} to 10^{-2} M. Subsequently, the electrode was employed to measure the response of solution containing primary anion (NaClO_4). This measurement process was conducted three times, with a new membrane utilized for one of the replicates. The studied interfering ions encompassed SCN^- , I^- , NO_2^- , NO_3^- , CO_3^{2-} , Br^- , Cl^- , CH_3COO^- , F^- , and SO_4^{2-} . The determination of selectivity coefficients for the primary anion (ClO_4^-) was performed using **Eq 2.1**. Subsequently, SCN^- , I^- , NO_2^- , NO_3^- , and Br^- were investigated as primary ions using the same methodology employed for ClO_4^- .

2.7 Membrane reversibility

The reversibility of the ion-selective electrode (ISE) was assessed by measuring the EMF of the ISE in a solution containing 10^{-3} M ClO_4^- . Subsequently, the ISE was rinsed with milli-Q water and immersed in a solution with a concentration of 10^{-2} M ClO_4^- . This cycle was repeated at least three times.

2.8 Effects of the solution pH

The pH of the solutions was systematically adjusted from 0 to 14 by gradually adding 0.01 M NaOH and HCl. The fabricated ion-selective electrode (ISE) was then utilized to measure the EMF of solutions containing 10^{-3} M and 10^{-2} M ClO_4^- , covering the entire pH range of 0-14.

2.9 Membrane reproducibility

Multiple membranes were fabricated using the same composition, consisting of 0.300 μmol of CoL, 60.0 mol% of TDMACl, 72.6 mg of PVC, and 145.2 mg of NPOE. The fabricated membranes were then subjected to potentiometric measurements to determine and compare their membrane characteristics.

2.10 Real sample analysis

We conducted tests on various brands of drinking water to assess their quality. The samples, including Purra and Sing, were obtained from Salaprakiew stores. To eliminate interfering ions in the samples, Sing and Purra were diluted 100 times using a mixture of sample and milli-Q water in a ratio of 0.2:19.8 ml. Subsequently, we investigated the potentiometric response and determined the concentration of ClO_4^- by comparing it to the potentiometric response of the milli-Q water after adding a known concentration of ClO_4^- .

2.11 Real-time analysis

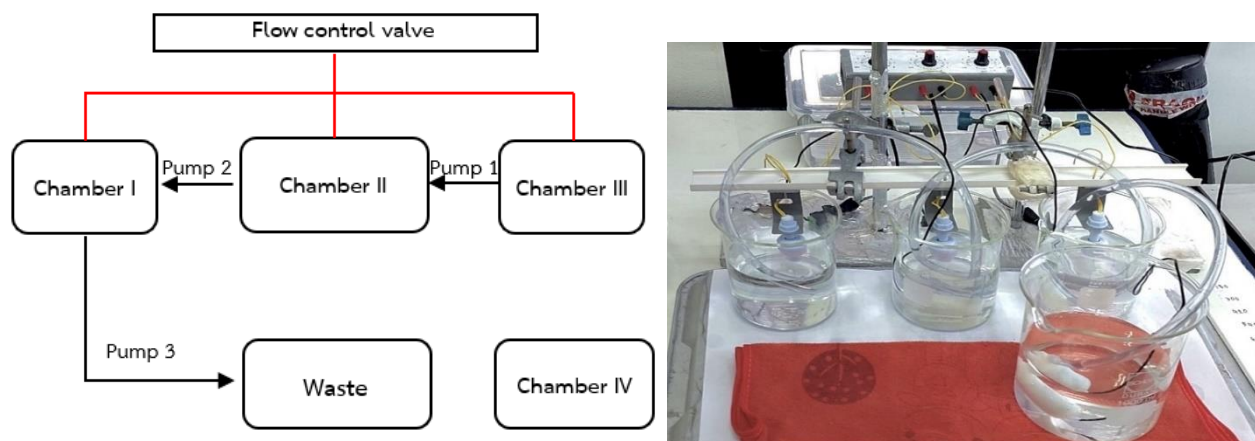


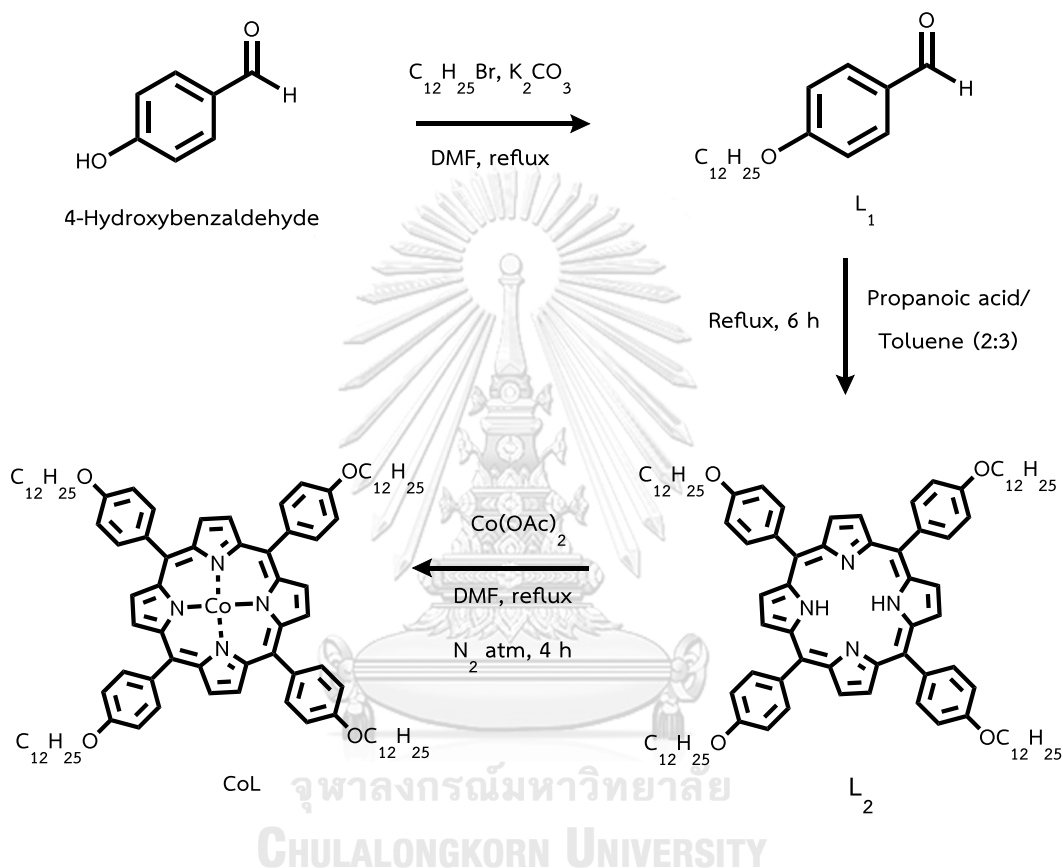
Figure 2.1 Experiment Setup for real-time analysis.

The simulation of water flow to replicate real situations, such as in rivers, storage tanks, and wastewater treatment ponds, was conducted using a pump, beaker, rubber tube, and flow control valve, as illustrated in **Figure 2.1**. Two fabricated Ion-Selective Electrodes (ISEs) were installed in two different positions. The first ISE was installed in chamber II, which was connected to the pumps and sample chambers I and III. Another ISE was installed in chamber IV, which contained Milli-Q water without ClO_4^- , serving as a control for monitoring the EMF signal. The potentiometric response of both the control and sample was measured simultaneously. Subsequently, $20 \mu\text{M}$ of $1.0 \times 10^{-4} \text{ M ClO}_4^-$ was added to the sample chamber to observe the decrease in the EMF signal compared to the control.

CHAPTER 3

RESULTS AND DISCUSSION

3.1 Synthesis and characterization of cobalt porphyrin (CoL)



Scheme 3.1 The synthesis of meso-tetra(4-alkyloxyphenyl) porphyrin cobalt complex (CoL)

The synthesis of the CoL compound was carried out in three steps as illustrated in **Scheme 3.1**. In the first step, 4-n-dodecyloxybenzaldehyde was reacted with 1-Bromododecane under reflux conditions. The resulting mixture was then subjected to extraction, washing, drying, and purification processes to obtain L_1 , a colorless oil, with a yield of 94%. L_1 was further characterized using $^1\text{H-NMR}$, $^{13}\text{C-NMR}$, and MALDI-TOF analyses. The $^1\text{H-NMR}$ spectrum revealed characteristic proton signals

of the aldehyde group at 9.78 ppm, aromatic protons at 7.73 ppm and 6.90 ppm, as well as long chain hydrocarbon protons at 3.94 ppm, 1.75-1.69 ppm, 1.41-1.18 ppm, and 0.80 ppm. The ^{13}C -NMR spectrum of compound L_1 exhibited ^{13}C signals at approximately 190.75 ppm, 164.32 ppm, 132.00 ppm, 129.81 ppm, 114.78 ppm, 68.46 ppm, 31.99 ppm, 29.73 ppm, 29.71 ppm, 29.66 ppm, 29.63 ppm, 29.42 ppm, 29.12 ppm, 26.03 ppm, 25.88 ppm, 22.76 ppm, and 14.18 ppm. Additionally, the MALDI-TOF mass analysis confirmed the structure of L_1 , displaying a prominent mass signal at m/z 290.22 (found: 290.435).

In the second step, L_1 , propanoic acid, and pyrrole were mixed under reflux conditions for 6 hours. Upon completion, the reaction mixture was cooled, filtered, washed, and recrystallized, resulting in the formation of dark-purple crystals (L_2) with a yield of 34%. L_2 was subsequently characterized using ^1H -NMR, ^{13}C -NMR, IR, UV-vis spectroscopy, and MALDI-TOF analysis. The ^1H -NMR spectrum exhibited proton signals of the pyrrole porphyrin at 8.87 ppm and 8.10 ppm, aromatic porphyrin at 7.26 ppm and 8.5 ppm, and alkyloxyphenyl at 4.23 ppm, 2.00-1.94 ppm, 1.62-1.32 ppm, 0.91 ppm, and -2.73 ppm. The ^{13}C -NMR spectrum of compound L_2 displayed ^{13}C signals at approximately 159.04 ppm, 135.69 ppm, 134.53 ppm, 119.91 ppm, 112.78 ppm, 68.41 ppm, 32.06 ppm, 29.83 ppm, 29.78 ppm, 29.64 ppm, 29.61 ppm, 29.50 ppm, 26.34 ppm, 22.82 ppm, and 14.25 ppm. Furthermore, the MALDI-TOF mass analysis supported the structure of L_2 , revealing a significant mass signal at m/z 1350.98 (found: 1350.679). The IR spectra of L_2 exhibited N-H stretching at 3314.47 cm^{-1} and alkyl C-H stretching at 2918.72 cm^{-1} and 2848.86 cm^{-1} . The UV-vis spectrum of L_2 in dichloromethane displayed bands around 423 nm, 502 nm, 557 nm, and 652 nm.

The final step involved preparing CoL by mixing L_2 and $\text{Co}(\text{OAc})_2$ under a nitrogen atmosphere and refluxing the mixture until the reaction was complete (4 hours). Following completion, the reaction mixture was purified and recrystallized, resulting in the formation of red crystals with a yield of 90%. The characterization of CoL was performed using MALDI-TOF and UV-vis spectroscopy. The MALDI-TOF mass analysis confirmed the structure of CoL, exhibiting an intense mass signal at m/z

1407.90 (found: 1407.935). The UV-vis spectrum of CoL in dichloromethane displayed bands around 416 nm and 531 nm.

3.2 Membrane preparation and optimization

We employed the prepared CoL as an ionophore in the fabrication of anion-selective electrodes and conducted a comprehensive study encompassing sensitivity, reproducibility, selectivity, and real sample analysis. Anion-selective electrodes possess specific desirable characteristics. Firstly, they should demonstrate stability in the response time trace line graph at equilibrium concentration, as depicted in **Figure 3.1**. Furthermore, the response slopes should closely approximate the theoretical Nernst slope of -59.2 mV/decade. This determination is achieved by calculating the average emf response for each analyte activity and establishing the calibration curve between $\log(a)$ and emf, as illustrated in **Figure 3.2**.

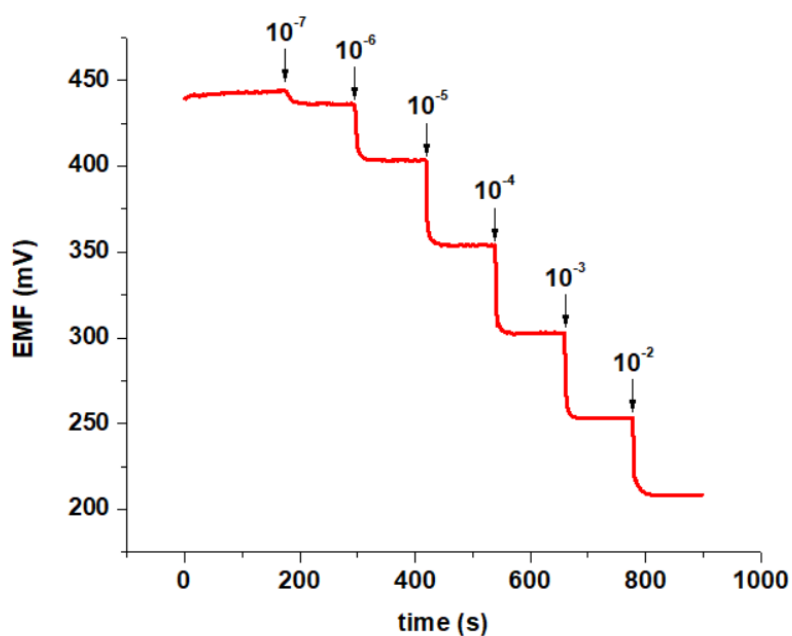


Figure 3.1 Time trace line of ISE after adding ClO_4^- (1.0×10^{-7} to 1.0×10^{-2} M) to the solution.

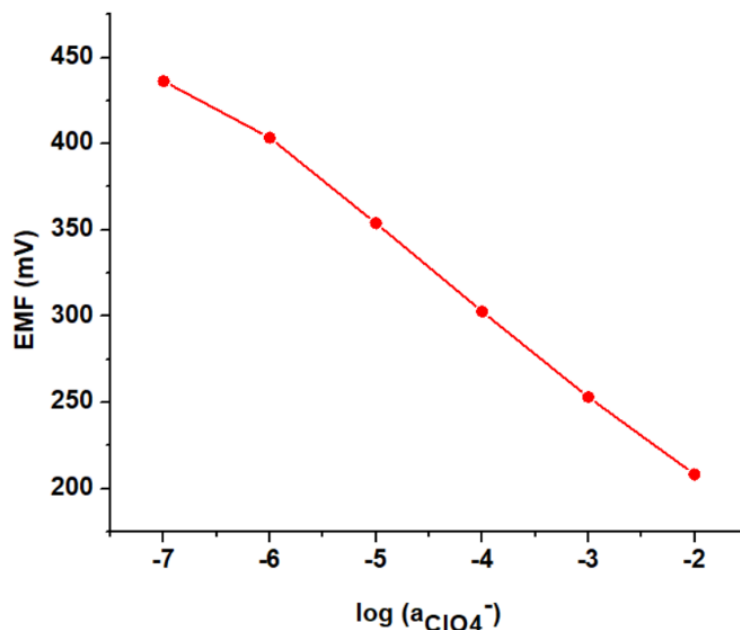


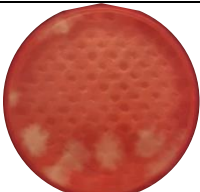



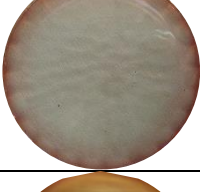

Figure 3.2 Calibration curve of average emf response for each analyte activity and $\log(a)$.

3.2.1 Optimized amount of ionophore for enhanced performance

The ion-selective membranes (ISMs) were prepared using a mixture of 33% polyvinylchloride (PVC), 66% 1-(2-Nitrophenoxy) octane (NPOE), and 1% each of CoL and tridodecylmethylammonium chloride (TDMACl). The concentration of the ionophore was systematically adjusted to determine the maximum amount that could be incorporated into the membrane while maintaining homogeneity. Increasing the ionophore amount enhances the probability of coordination between the ionophore and the targeted anion. **Table 3.1** displays the membranes prepared using different amounts of ionophore. Membranes No. 1 to 3, containing 1.2 μmol , 1.4 μmol , and 1.8 μmol of ionophore, respectively, exhibited non-homogeneity based on the physical appearance of the membranes. Membrane no.1 displayed ionophore leakage after drying due to an excessive amount of ionophore, resulting in overcapacity that could not dissolve. Membrane No. 2 exhibited aggregates of CoL crystals positioned at the center of the membrane. Membrane no.3 showed red

crystal colonies of CoL on the membrane surface. Such non-homogeneity in the membranes hinders the proper binding between the ionophore and anions, leading to reduced sensitivity of the ISE. Conversely, membranes no.4 to 6, with 0.1 μmol , 0.2 μmol , and 0.3 μmol of ionophore, respectively, demonstrated homogeneous properties.

Table 3.1 Composition of membrane components and membrane appearance.

No.	PVC (mg)	NPOE (mg)	CoL (μmol)	TDMACl (mol% compared to CoL)	Physical appearance
1	72.6	145.2	1.2	20.0	
2	72.6	145.2	1.4	60.0	
3	72.6	145.2	1.8	60.0	
4	72.6	145.2	0.1	60.0	
5	72.6	145.2	0.2	60.0	
6	72.6	145.2	0.3	60.0	

3.2.2 Optimization of amount of ionophore to the enhanced the performance of membrane

In order to optimize the composition of the membrane, various compositions were prepared by systematically adjusting the proportions of the ionophore (CoL) and the cationic additive (TDMACl). The objective was to identify the optimal combination that would enhance the membrane performance.

Initially, the ionophore amount was adjusted within the range of 0.1 to 0.3 μmol while keeping the proportions of PVC, NPOE, and TDMACl constant. The TDMACl, or cationic additive, was maintained at a fixed ratio of 20 mol% relative to the amount of ionophore for membrane No. 4-6. This approach was adopted to mitigate any potential influence of the cationic additive on the behavior of anions. Excessive amounts of the cationic additive can facilitate binding with the ions, ultimately leading to reduced membrane selectivity.

Then, the properties of membranes No. 4-6 were assessed by measuring the potentiometric response to various anions. The results are presented in **Figure 3.3**, which exhibits the relationship between the logarithm of anion activity and the corresponding potential response. Among the tested membranes, the one composed of 0.3 μmol of ionophore, membrane No.6, exhibited a favorable calibration curve with a broader concentration range. Additionally, it exhibited an emf response that is close to the theoretical Nernst slope of approximately 59.2 mV/decade for all anions, as shown by the slope and the membrane composition presented in **Table 3.2**. According to the results, it was observed that the potentiometric response was highest with the greatest quantity of ionophore. This can be attributed to the ionophore's role as an anion carrier, facilitating the transfer of anions from the aqueous solution to the membrane phase. Moreover, an increased amount of ionophore resulted in an improved potential response.

Table 3.2 The difference amount of ionophore and potentiometric response toward different anions.

No.	PVC (mg)	NPOE (mg)	CoL (μmol)	TDMACl (mol%)	Slope (mV/decade)				
					ClO_4^-	SCN^-	NO_3^-	Br^-	I^-
4	72.6	145.2	0.1	20.0	-41.7	-38.1	-40.5	-21.0	-38.1
5	72.6	145.2	0.2	20.0	-46.9	-22.5	-42.1	-30.8	-43.6
6	72.6	145.2	0.3	20.0	-51.6	-46.5	-44.6	-53.9	-53.7

*** mol% of TDMACl compared to CoL

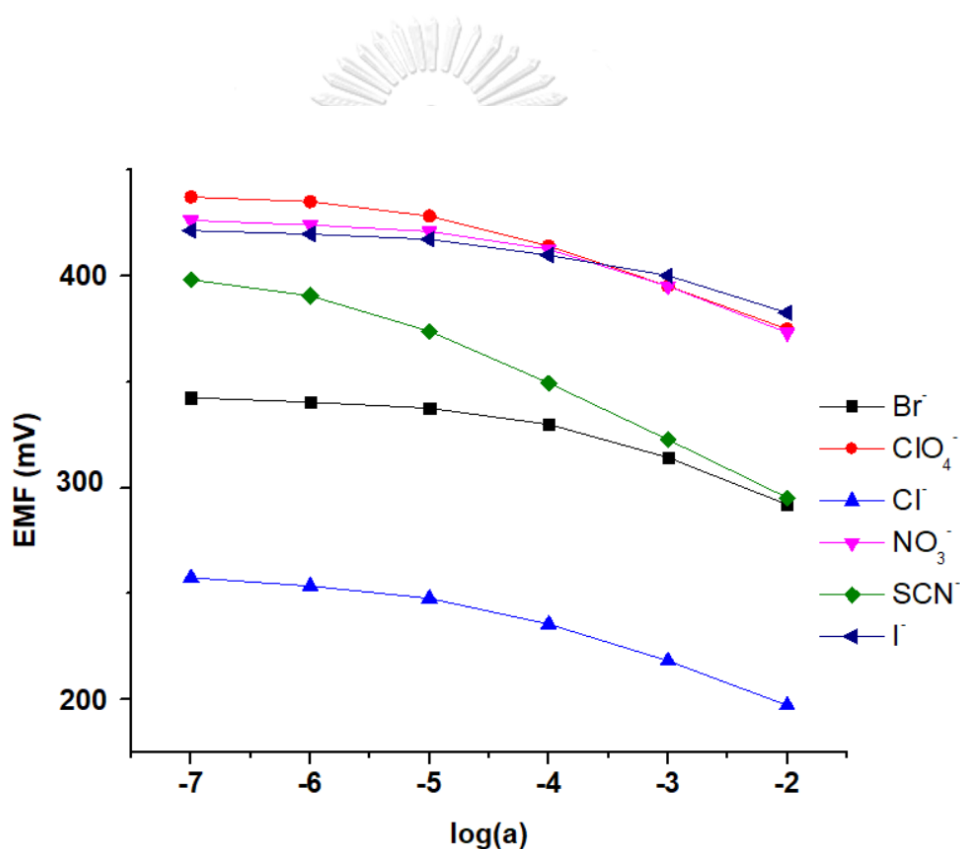


Figure 3.3 Potentiometric response (emf) of anions with 0.3 μmol CoL and 20 mol% TDMACl.

The amount of TDMACl was subsequently adjusted to 20, 40, and 60 mol% relative to the CoL concentration, while maintaining the proportions of PVC, NPOE, and 0.3 μmol of CoL constant. In order to prevent any detrimental effects on the behavior of the anions, careful control was exercised over the quantity of the

cationic additive. As mentioned earlier, the potentiometric response was subsequently tested. The outcomes of these evaluations are graphically depicted in **Figure 3.4**, **Figure 3.5**, and **Figure 3.6**, illustrate the potentiometric responses of the three anions (ClO_4^- , SCN^- , and NO_3^-). Among the membranes tested, the one composed of 0.3 μmol of ionophore and 60 mol% of TDMACl, membrane No.9, demonstrated the most favorable calibration curve and potentiometric response. Furthermore, it exhibited a potentiometric response closest to the theoretical Nernst slope, as shown in **Table 3.3**, with values of -53.9, -57.6, -53.7, -54.2, and -58.1 mV/decade towards Br^- , ClO_4^- , I^- , NO_3^- , and SCN^- , respectively. The incorporation of the cationic additive (TDMACl) contributed to enhanced ion exchanger kinetics and ionic mobility within the membrane matrix, leading to improved sensitivity in the potentiometric response. Therefore, an increased amount of the cationic additive resulted in a better potentiometric response. Consequently, the optimal ratio of membrane components was determined to be 0.300 μmol of CoL, 60.0 mol% of TDMACl, 72.6 mg of PVC, and 145.2 mg of NPOE.

Figure 3.7 illustrates the potentiometric response observed in the fabricated ion-selective electrode (ISE) when exposed to various anions, namely ClO_4^- , SCN^- , NO_3^- , Br^- , I^- , Cl^- , CH_3COO^- , Cl^- , CO_3^{2-} , F^- , and SO_4^{2-} . It is evident from the calibration curve that ClO_4^- exhibits the most extensive linear range, ranging from 10^{-6} to 10^{-2} , surpassing the other anions. Following closely behind, SCN^- also demonstrates a favorable potentiometric response. Notably, ClO_4^- and SCN^- both exhibit desirable performance within the concentration range of 1.00×10^{-6} to 1.00×10^{-2} M, with detection limits of 2.13×10^{-6} and 2.56×10^{-6} M, respectively.

Table 3.3 The difference amount of TDMACl and potentiometric response toward different anions

No.	PVC (mg)	NPOE (mg)	CoL (μmol)	TDMACl (mol%)	Slope (mV/decade)					
					ClO_4^-	SCN^-	NO_3^-	Br^-	I^-	Cl^-
7	72.6	145.2	0.3	20.0	-41.1	-52.4	-20.5	-29.7	-47.1	N/A
8	72.6	145.2	0.3	40.0	-51.7	-54.3	-49.2	-48.8	-37.6	N/A
9	72.6	145.2	0.3	60.0	-57.6	-58.1	-54.2	-53.9	-53.7	N/A

*** mol% of TDMACl compared to CoL

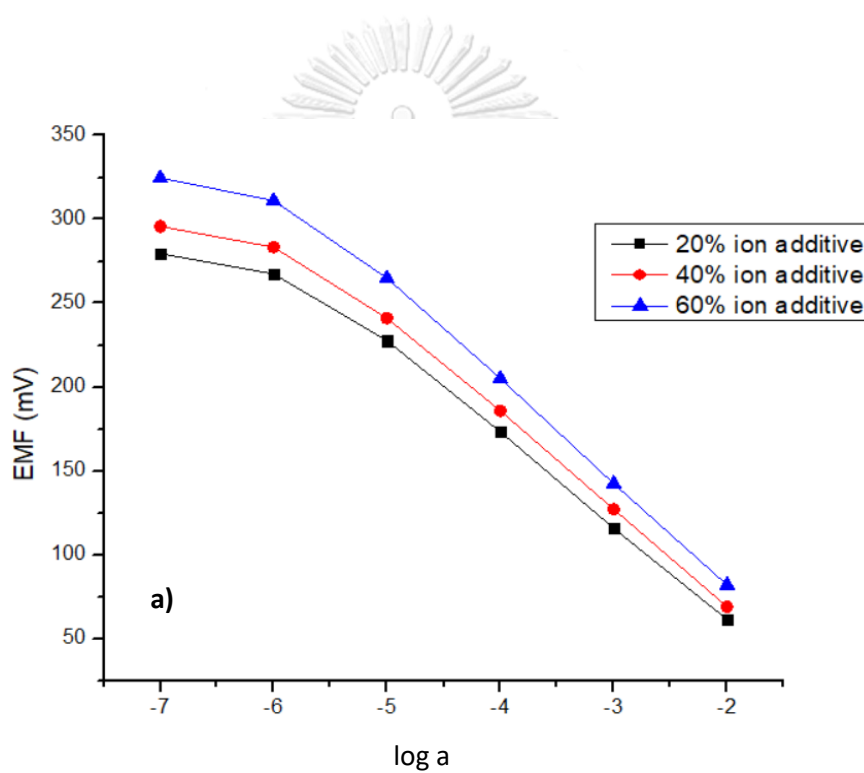


Figure 3.4 Potentiometric response with difference amount of cationic additive toward SCN^- .

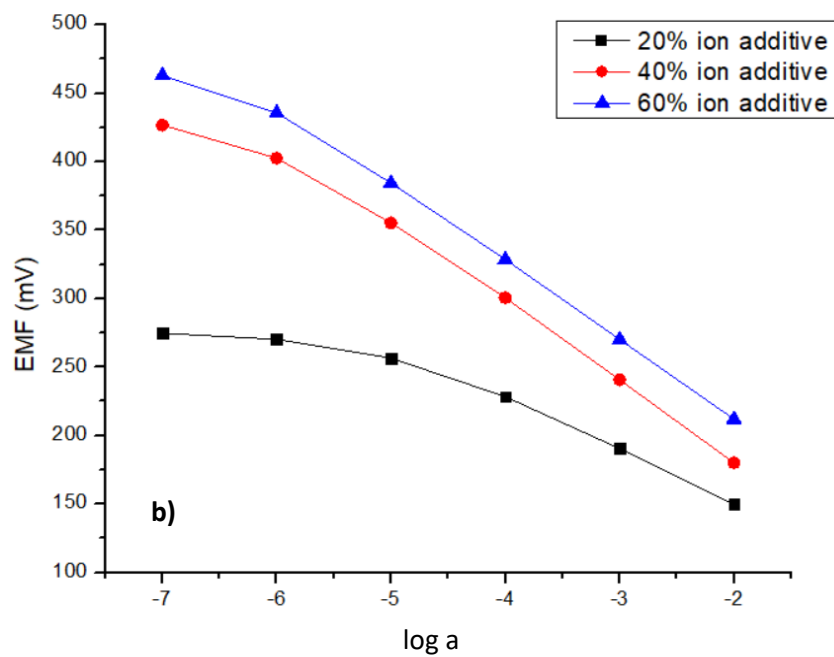


Figure 3.5 Potentiometric response with difference amount of cationic additive toward ClO_4^- .

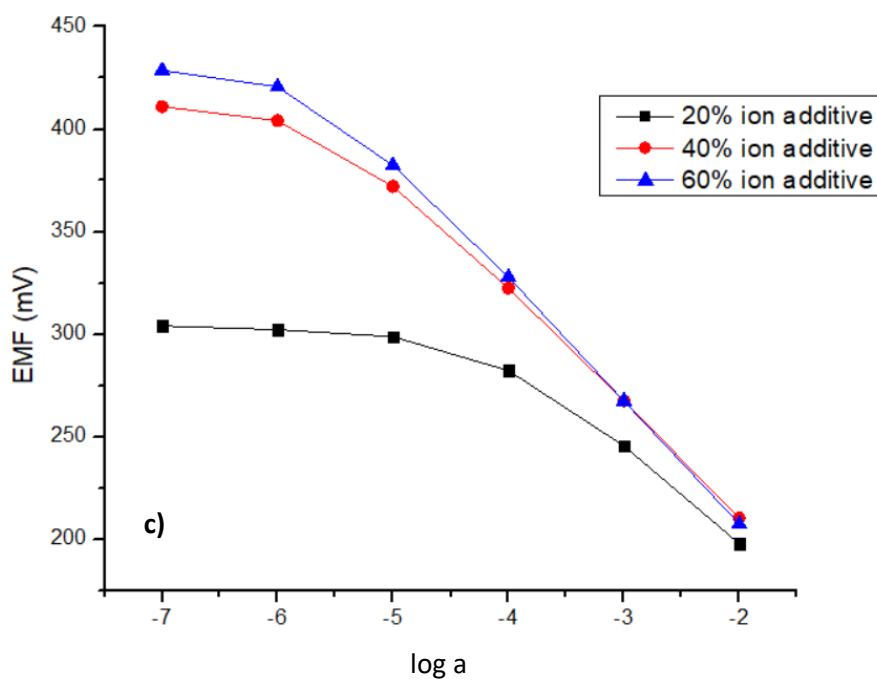


Figure 3.6 Potentiometric response with difference amount of cationic additive toward NO_3^- .

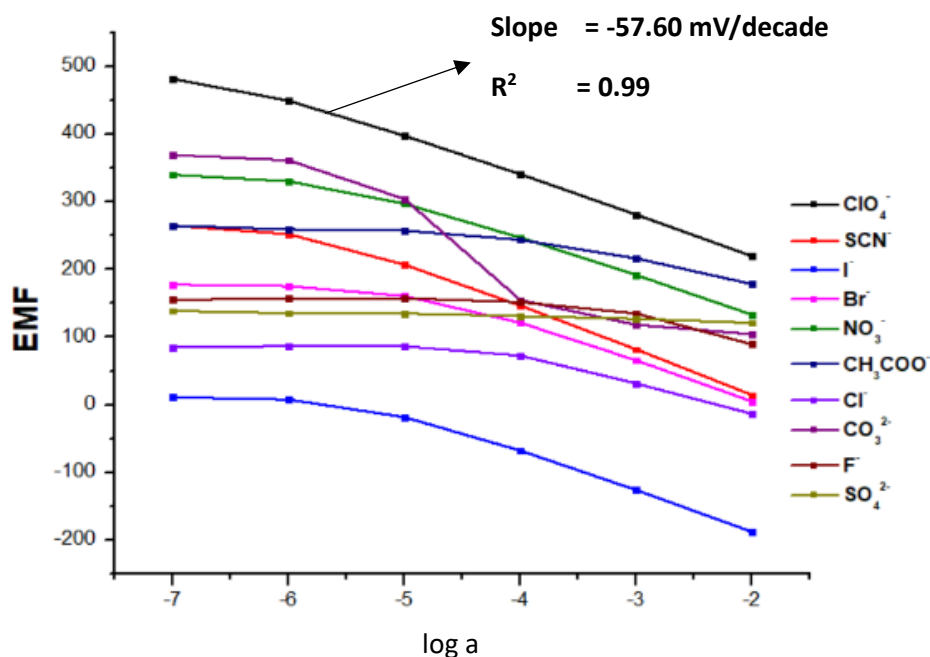


Figure 3.7 Potentiometric response (emf) of anions with 0.3 μmol CoL and 60 mol% TDMACl.

3.3 Membrane Performance

3.3.1 Membrane Selectivity

The selectivity of an ionophore is a critical characteristic in the context of an ISE. It is of utmost importance that the ionophore exhibits a high degree of selectivity towards the target analyte, thereby avoiding any potential bias resulting from interference by other ions. The selectivity of the ionophore arises from the formation of complexes between the ionophore and the analyte ions. In order to assess the selectivity of ISEs, the "unbiased selectivity coefficient" concept, as proposed by Bakker and collaborators, is employed. This approach enables a comprehensive evaluation of the selectivity performance of the ionophore in the ISE system.⁵⁹ In order to evaluate the selectivity of the ion-selective electrode towards a range of 10 different anions, including ClO_4^- , SCN^- , I^- , NO_2^- , NO_3^- , CO_3^{2-} , Br^- , Cl^- , CH_3COO^- , F^- , and SO_4^{2-} , we conducted a detailed investigation into the potentiometric selectivity coefficients. These coefficients, denoted as $\log K_{\text{pot}}(i,j)$, were determined by

comparing the response of the primary ion (perchlorate) to that of the interfering ions present in the solutions. The determination process involved employing the separate solution method (SSM). **Table 3.4** shown the potentiometric selectivity coefficient of the fabricated ISEs when SCN^- , NO_3^- , I^- , and ClO_4^- are primary ions. The selectivity coefficient found to be $\text{ClO}_4^- > \text{SCN}^- > \text{I}^- > \text{NO}_2^- > \text{NO}_3^- > \text{CO}_3^{2-} > \text{Br}^- > \text{Cl}^- > \text{CH}_3\text{COO}^- > \text{F}^- > \text{SO}_4^{2-}$. The potentiometric selectivity coefficient of ClO_4^- ($\log K_{\text{ClO}_4^-, \text{X}^-} = 0.00$, $\log K_{\text{SCN}^-, \text{X}^-} = 1.08$, $\log K_{\text{NO}_3^-, \text{X}^-} = 2.96$, and $\log K_{\text{I}^-, \text{X}^-} = 1.74$) are the highest among other anions.

Table 3.4 Selectivity coefficients of anions

X^-	ClO_4^-	SCN^-	I^-	Br^-	NO_3^-	CH_3COO^-	Cl^-	CO_3^{2-}	F^-	SO_4^{2-}
$\log K_{\text{ClO}_4^-, \text{X}^-}$	0.00	-0.79	-1.11	-3.76	-3.02	-4.42	-4.19	-3.67	-4.85	-6.76
$\log K_{\text{SCN}^-, \text{X}^-}$	1.08	0.00	-0.24	-2.52	-1.83	-3.39	-3.42	-2.31	-3.82	-5.86
$\log K_{\text{NO}_3^-, \text{X}^-}$	2.96	2.21	1.18	-0.71	0.00	-1.78	-1.48	-0.99	-2.25	-4.00
$\log K_{\text{I}^-, \text{X}^-}$	1.74	0.83	0.00	-1.75	-1.03	-2.53	-2.24	-1.38	-3.52	-4.96

The logarithm of the potentiometric stability constant ($\log K_{ij}^{\text{pot}}$) for ClO_4^- remains the highest compared to other anions, despite all anions being considered primary ions. **Figure 3.8** shows the distinctive potentiometric response characteristics of ClO_4^- in comparison to SCN^- , as indicated by the time trace line. It is evident that the emf response of ClO_4^- is lower than that of SCN^- . Consequently, the fabricated membrane exhibits higher sensitivity and selectivity towards ClO_4^- compared to SCN^- and other anions. The fabricated ion-selective electrode (ISE) exhibits selectivity towards ClO_4^- due to two primary factors. Firstly, the increased steric hindrance of the substituents on CoL enhances its lipophilicity, favoring preferential interaction with the lipophilic ClO_4^- among other anions. Secondly, the coordination number of CoL is well-suited for coordinating with ClO_4^- .

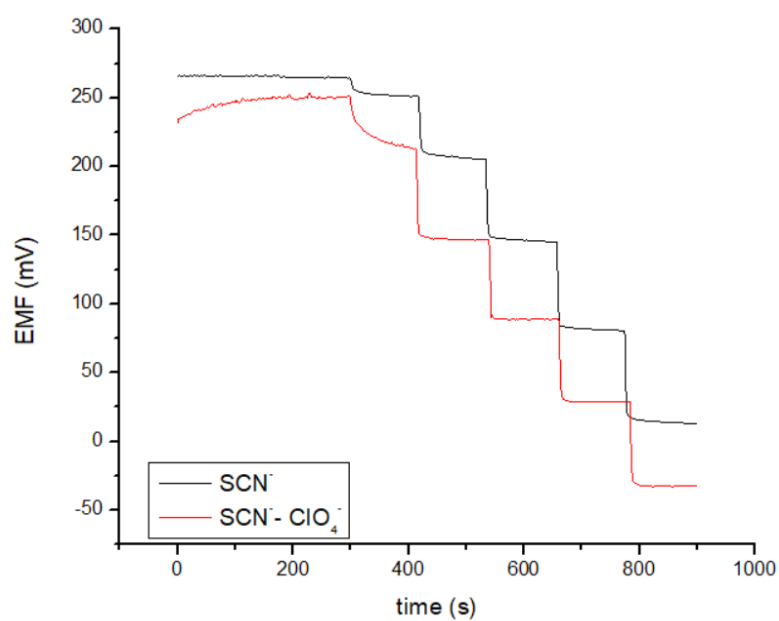


Figure 3.8 EMF response of the SCN^- and substituted with ClO_4^- .



3.3.2 pH effect

The influence of solution pH was evaluated by adjusting its levels from 2 to 13 using HCl and NaOH. The fabricated membrane was utilized to measure the solution, which contained concentrations of 1.0×10^{-2} M and 1.0×10^{-3} M of ClO_4^- , as showed in **Figure 3.9**. Despite variations in the solution's pH, the membrane exhibited consistent EMF responses. Based on this observation, we can conclude that the fabricated membrane is capable of accurately determining ClO_4^- concentrations across a wide pH range of 2 to 13, with no significant changes in EMF values. However, the fabricated membrane was affected when the pH fell below 2 or exceeded 13, due to the higher concentration of interfering Cl^- and OH^- ions from the excessive use of HCl and NaOH to adjust the pH of the solution. However, the study revealed a sufficiently wide effective pH range for the sample, rendering critical pH adjustments unnecessary.

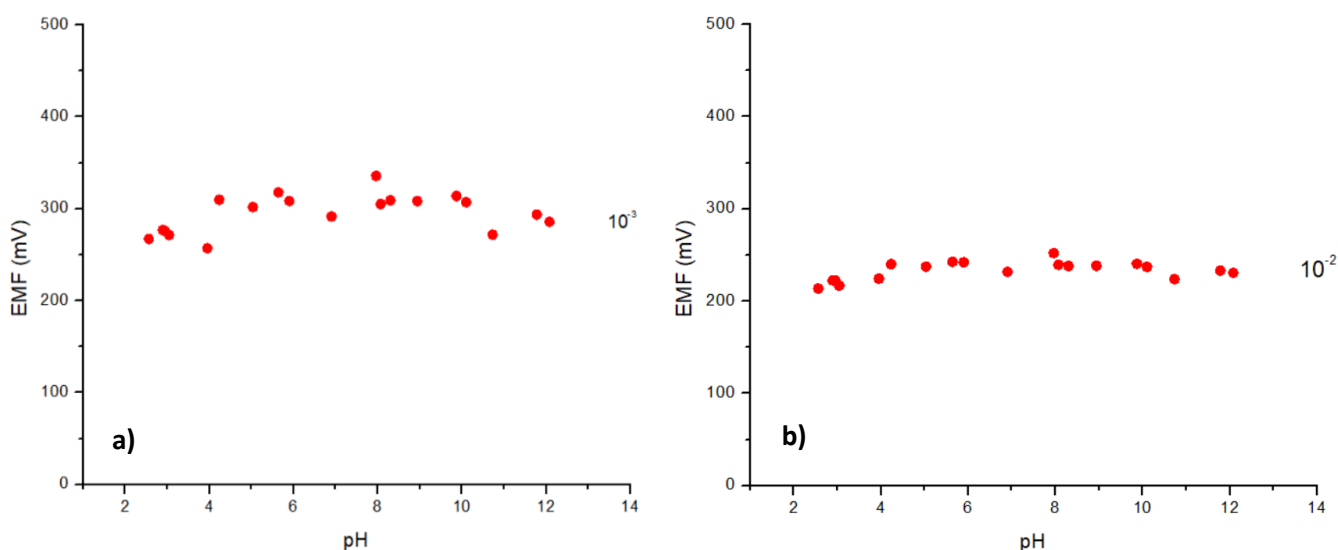


Figure 3.9 Potential response of the fabricated ISE with the difference pH

a) 10^{-2} M of ClO_4^- and b) 10^{-3} M of ClO_4^- .

3.3.3 Membrane reversibility

The reversibility of the fabricated membrane is an important property of the ISE. **Figure 3.10** illustrates the potentiometric response or time trace line of the ISE when measuring solutions with varying amounts of ClO_4^- . As observed, the emf signal remains highly stable when the solution concentration is changed from 1.0×10^{-3} to 1.0×10^{-2} . Additionally, the emf signal can be consistently restored for the same concentration of ClO_4^- in each cycle. Consequently, the fabricated membrane demonstrates excellent reversibility and can be effectively employed for measuring the concentration of ClO_4^- . The time trace line of the solution after the addition of ClO_4^- is depicted in **Figure 3.1** and **Figure 3.2**. Notably, the fabricated membrane demonstrates a remarkably rapid response time in achieving a stable emf signal.

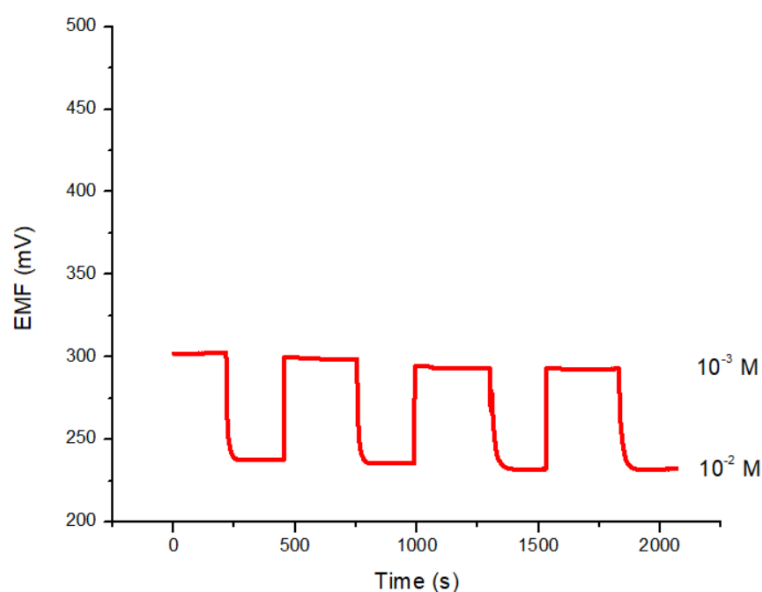


Figure 3.10 Reversibility of ISE at the concentration between 1.0×10^{-3} and 1.0×10^{-2} M.

3.3.4 Membrane reproducibility

The reproducibility of the ion-selective electrode (ISE) is a critical characteristic to evaluate. In this study, we examined the potentiometric response of the membrane that was prepared using a composition of 0.300 μmol of CoL, 60.0 mol% of TDMACl, 72.6 mg of PVC, and 145.2 mg of NPOE. To assess reproducibility, multiple membranes with identical compositions were fabricated, and the potentiometric response of ClO_4^- was measured. The results indicated that the response slopes for ClO_4^- showed only slight variations, approximately 57.6 ± 2 mV/decade, across different measurement times and membranes. These findings indicated that the fabricated ISE exhibited good reproducibility.

3.3.5 Real sample analysis

The final aspect of evaluating the membrane performance involved the application of the fabricated ion-selective electrode (ISE) to determine the concentration of perchlorate in real samples. In this study, we conducted tests on various brands of drinking water to assess their quality. The water samples, specifically Purra and Sing, were obtained from Salaprakiew stores. Initially, our investigation focused on the determination of perchlorate anions in tap water. We performed two calibration measurements using Milli-Q water and then switched to Sing water. However, it was observed that Sing water could not be directly determined due to interference. To overcome this, Sing water was diluted 100 times with Milli-Q water to eliminate the interference. Subsequently, known concentrations of ClO_4^- within the range of 1.0×10^{-6} to 1.0×10^{-3} M were spiked into the diluted Sing water. An example analysis demonstrating this process is depicted in **Figure 3.11**. Similar experiments were conducted using Purra water, as shown in **Figure 3.12**. The emf value, concentration, % recovery, and measurement data of ClO_4^- in both Sing and Purra water were calculated using the calibration curve equation. These results are presented in the accompanying **Table 3.5**.

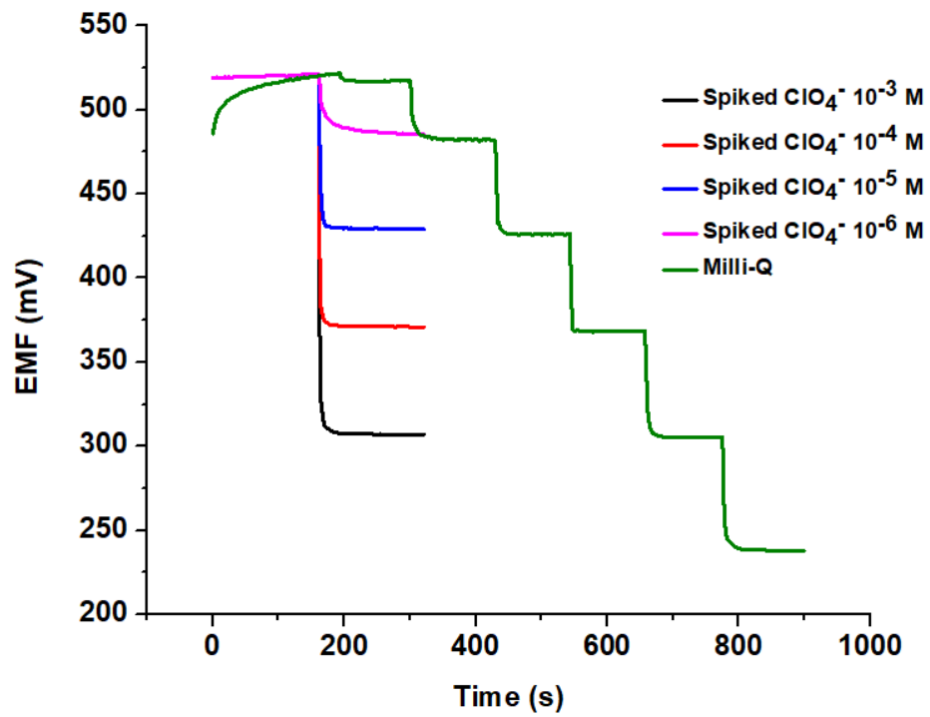


Figure 3.11 An example of Sing (drinking water) analysis.

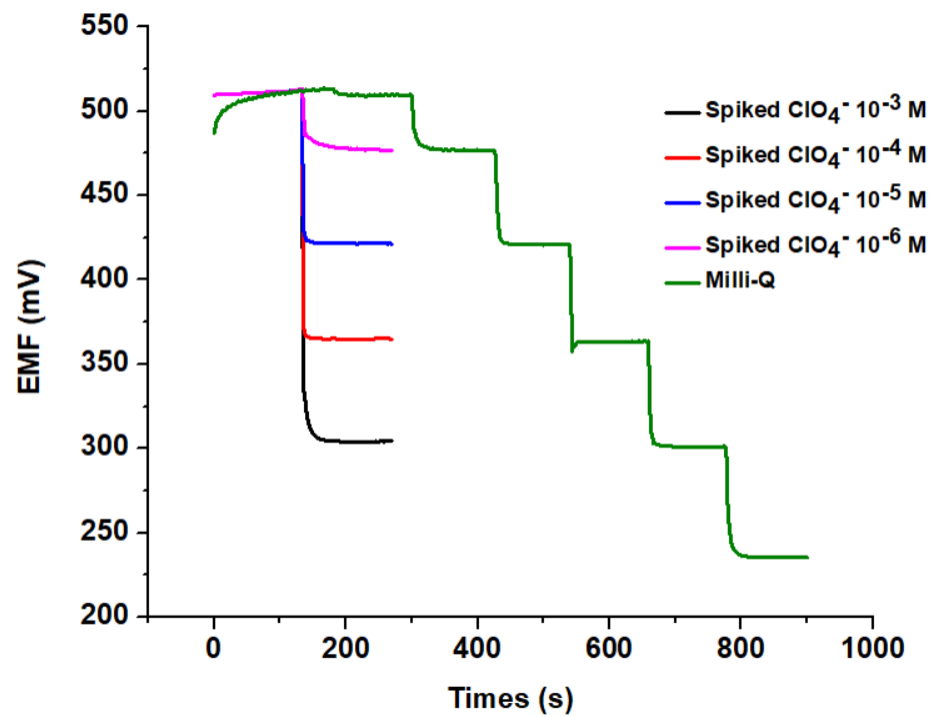


Figure 3.12 An example of Purra (drinking water) analysis.

Table 3.5 Calculation data of perchlorate selective electrode for real samples.

Samples	Spiked (M)	Found (M)	% recovery	S.D.	R.S.D.
Sing	1.00×10^{-6}	9.99×10^{-7}	99.93	2.98	2.99
	1.00×10^{-5}	1.01×10^{-6}	101.35	5.10	5.03
	1.00×10^{-4}	9.70×10^{-5}	96.98	3.43	3.53
	1.00×10^{-3}	9.22×10^{-4}	92.23	1.56	1.69
Purra	1.00×10^{-6}	1.06×10^{-6}	106.26	13.87	13.06
	1.00×10^{-5}	7.45×10^{-6}	102.92	9.14	8.88
	1.00×10^{-4}	9.79×10^{-5}	97.90	8.49	8.67
	1.00×10^{-3}	9.63×10^{-4}	96.29	3.63	3.77

After conducting multiple measurements of the ClO_4^- in two water samples, we have identified the sensor performances that yielded the best results for each concentration. Subsequently, we calculated the average concentration and percentage recovery. The collected measurement data, percentage recovery, standard deviation (S.D.), and relative standard deviation (R.S.D.) of the real water samples are presented in **Table 3.5**. Based on the findings provided in **Table 3.5**, it can be inferred that our sensors demonstrate satisfactory performance across three different concentrations in both types of actual water samples.

3.4 Real-time analysis

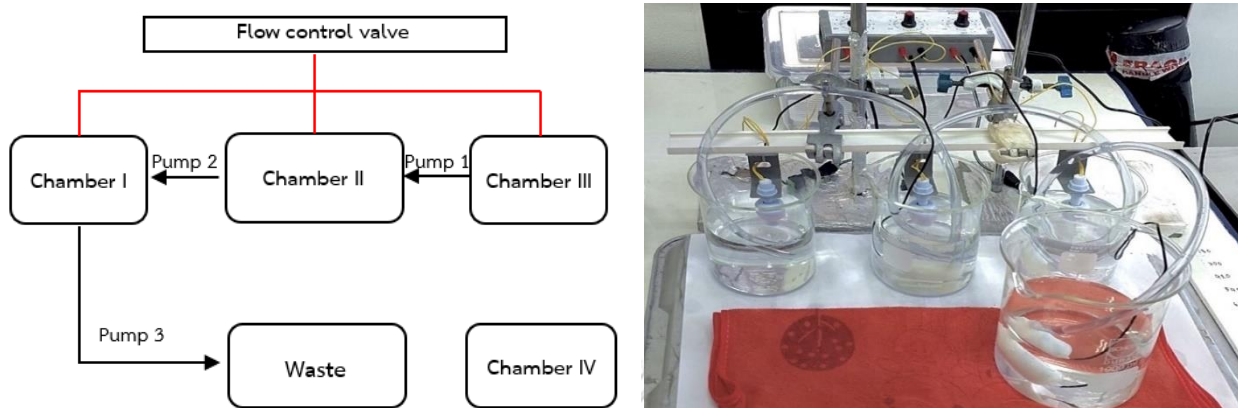


Figure 3.13 Experiment Setup for real-time analysis.



Figure 3.14 The emf signal of two fabricated ISEs for real-time analysis.

According to **Figure 3.13**, an experimental apparatus was constructed to simulate the flow of water in a genuine water source, such as a natural water source or an industrial wastewater system with continuous flow. Electrodes were installed at two specific locations for measurement purposes: a chamber IV, designated as the control chamber for water without toxic or perchlorate ions, and another electrode placed in the region simulating the water flow (referred to as chamber I to III). Upon installation, the operation of both electrodes commenced. Initially, the signal characteristics were inconsistent, necessitating a waiting period for the signals to stabilize, as depicted in **Figure 3.14**. This stabilization phase occurred between 700 and 1100 seconds, during which the EMF signal represented by the pink line exhibited no significant change in EMF value compared to the red EMF signal (control electrode). This lack of change was attributable to the absence of perchlorate ions.

Subsequently, experiments were conducted by introducing ClO_4^- into the control chamber and chambers I to III, simulating the flow of water. This led to a modification in the EMF signal characteristics. The signal displayed lower values compared to the control electrode due to the presence of ClO_4^- contamination. This alteration was observed between 1100 and 1400 seconds. The fabricated ISE demonstrated selectivity in analyzing ClO_4^- within a concentration range of 1.0×10^{-6} to 1.0×10^{-2} , with a minimum detectable concentration of $2.56 \mu\text{M}$. It is crucial to note that perchlorate ion contamination in drinking water is considered hazardous when surpassing $0.11 \mu\text{M}$ (United State Environment Protection Agency; US EPA). Consequently, when utilizing this experimental device in practical applications, a decline in the pink EMF signal would indicate the existence of ClO_4^- contamination in the analyzed sample at a potentially hazardous level (greater than $0.11 \mu\text{M}$).

CHAPTER 4

CONCLUSION

The ionophore CoL has been synthesized in 90 %yield. Physical methods such as $^1\text{H-NMR}$, $^{13}\text{C-NMR}$, and MALDI-TOF, supported CoL structure and purity. The optimal ion selective membrane composition was 0.300 μmol of CoL, 60.0 mol% of TDMACl, 72.6 mg of PVC, and 145.2 mg of NPOE. The fabricated ISEs incorporating CoL as the ionophore exhibited a potentiometric response of -57.6 mV/decade ($R^2 = 0.99$), close to the theoretical Nernst slope, in a concentration range of 1.00×10^{-6} to 1.00×10^{-2} M for ClO_4^- . The detection limit was determined to be 2.13×10^{-6} M.

The fabricated ISEs exhibited the highest selectivity coefficient for ClO_4^- , highlighting their specificity towards this particular ion. The performance of the ISEs was thoroughly evaluated in terms of pH stability, reversibility, and reproducibility. The membranes exhibited consistent EMF responses across a wide pH range of 2 to 13. The ISEs also demonstrated excellent reversibility and rapid response times, ensuring reliable and efficient measurements.

Furthermore, the application of the fabricated ISEs to real water samples, including various brands of drinking water, showed satisfactory performance. In addition, the fabricated ISEs showed promising performance characteristics for the real-time monitoring and analysis of ClO_4^- in water samples. Further experiments may focus on improving the limit of detection of the ISEs to levels below the hazardous threshold, thereby augmenting the efficiency of real-time analysis. In addition, to mitigate the impact of interfering ions such as SCN^- , it is necessary to eliminate their presence prior to measuring the EMF signals. One effective approach is the utilization of a marking reagent to facilitate their removal before the measurement process.

REFERENCES

1. Mohammad, A.; Chahar, J. P. S., Thin-layer chromatographic separation, colorimetric determination and recovery of thiocyanate from photogenic waste, river and sea waters. *Journal of Chromatography A* **1997**, *774* (1), 373-377.
2. Spurr, L. P.; Watts, M. P.; Gan, H. M.; Moreau, J. W., Biodegradation of thiocyanate by a native groundwater microbial consortium. *PeerJ* **2019**, *7*, e6498.
3. Urbansky, E. T., Perchlorate as an environmental contaminant. *Environ Sci Pollut Res Int* **2002**, *9* (3), 187-92.
4. Willemin, M. E.; Lumen, A., Thiocyanate: a review and evaluation of the kinetics and the modes of action for thyroid hormone perturbations. *Crit Rev Toxicol* **2017**, *47* (7), 537-563.
5. Carrasco, N., Iodide transport in the thyroid gland. *Biochimica et Biophysica Acta (BBA) - Reviews on Biomembranes* **1993**, *1154* (1), 65-82.
6. Naik, R. M.; Kumar, B.; Asthana, A., Kinetic spectrophotometric method for trace determination of thiocyanate based on its inhibitory effect. *Spectrochimica Acta Part A: Molecular and Biomolecular Spectroscopy* **2010**, *75* (3), 1152-1158.
7. Basova, E. M.; Ivanov, V. M.; Apendeeva, O. K., Spectrophotometric determination of thiocyanate ions in stratal waters. *Moscow University Chemistry Bulletin* **2014**, *69* (1), 12-19.
8. Bhandari, R. K.; Manandhar, E.; Oda, R. P.; Rockwood, G. A.; Logue, B. A., Simultaneous high-performance liquid chromatography-tandem mass spectrometry (HPLC-MS-MS) analysis of cyanide and thiocyanate from swine plasma. *Analytical and Bioanalytical Chemistry* **2014**, *406* (3), 727-734.
9. Ammazzini, S.; Onor, M.; Pagliano, E.; Mester, Z.; Campanella, B.; Pitzalis, E.; Bramanti, E.; D'Ulivo, A., Determination of thiocyanate in saliva by headspace gas chromatography-mass spectrometry, following a single-step aqueous derivatization with triethyloxonium tetrafluoroborate. *Journal of Chromatography A* **2015**, *1400*, 124-130.
10. Amemiya, S., *Potentiometric Ion-Selective Electrodes*. Elsevier: Amsterdam, 2007; p 261-294.

11. Lvova, L.; Verrelli, G.; Stefanelli, M.; Nardis, S.; Di Natale, C.; Amico, A. D.; Makarychev-Mikhailov, S.; Paolesse, R., Platinum porphyrins as ionophores in polymeric membrane electrodes. *Analyst* **2011**, *136* (23), 4966-4976.
12. Baek, J.-G., & Kim, Jin-San, The Composition Dependence Selectivity Changes by Plasticizer at the Cation Sensors Based on Tetracycline Antibiotics. *Bulletin of the Korean Chemical Society* **2008**, *29*, 165-167.
13. Masih, D.; Aly, S. M.; Alarousu, E.; Mohammed, O. F., Photoinduced Triplet-State Electron Transfer of Platinum Porphyrin: a One-Step Direct Method for Sensing Iodide with an Unprecedented Detection Limit. *Journal of Materials Chemistry A* **2015**, *3* (13), 6733-6738.
14. Paolesse, R.; Nardis, S.; Monti, D.; Stefanelli, M.; Di Natale, C., Porphyrinoids for Chemical Sensor Applications. *Chemical Reviews* **2017**, *117* (4), 2517-2583.
15. Carey, C., Plasticizer Effects in the PVC Membrane of the Dibasic Phosphate Selective Electrode. *Chemosensors (Basel)* **2015**, *3* (4), 284-294.
16. Joon, N. K.; Barnsley, J. E.; Ding, R.; Lee, S.; Latonen, R.-M.; Bobacka, J.; Gordon, K. C.; Ogawa, T.; Lisak, G., Silver(I)-selective electrodes based on rare earth element double-decker porphyrins. *Sensors and Actuators B: Chemical* **2020**, *305*, 127311.
17. Kou, L., Detection of Bromide Ions in Water Samples with a Nanomolar Detection Limit using a Potentiometric Ion-selective Electrode. *International Journal of Electrochemical Science* **2019**, *14*, 1601-1609.
18. Lascu, A.; Plesu, N.; Anghel, D.; Birdeanu, M. I.; Dana, V.; Fagadar-Cosma, E., Optical Detection of Bromide Ions Using Pt(II)-5,10,15,20-Tetra-(4-methoxy-phenyl)-porphyrin. *Chemosensors* **2019**, *7*.
19. Pietrzak, M.; Meyerhoff, M. E., Polymeric Membrane Electrodes with High Nitrite Selectivity Based on Rhodium(III) Porphyrins and Salophens as Ionophores. *Analytical Chemistry* **2009**, *81* (9), 3637-3644.
20. Vlascici, D.; Fagadar-Cosma, E.; Pica, E. M.; Cosma, V.; Bizerea, O.; Mihailescu, G.; Olenic, L., Free Base Porphyrins as Ionophores for Heavy Metal Sensors. *Sensors* **2008**, *8* (8), 4995-5004.
21. Wirojsaengthong, S.; Aryuwananon, D.; Aeungmaitrepirom, W.; Pulpoka, B;

- Tuntulani, T., A colorimetric paper-based optode sensor for highly sensitive and selective determination of thiocyanate in urine sample using cobalt porphyrin derivative. *Talanta* **2021**, *231*, 122371.
22. Descalzo, A. B.; Martínez-Mañez, R.; Sancenón, F.; Hoffmann, K.; Rurack, K., The Supramolecular Chemistry of Organic–Inorganic Hybrid Materials. *Angewandte Chemie International Edition* **2006**, *45* (36), 5924-5948.
23. Vlascici, D.; Fagadar-Cosma, E.; Popa, I.; Chiriac, V.; Gil-Agusti, M., A novel sensor for monitoring of iron(III) ions based on porphyrins. *Sensors (Basel)* **2012**, *12* (6), 8193-203.
24. Srinivasan, A.; Viraraghavan, T., Perchlorate: health effects and technologies for its removal from water resources. *Int J Environ Res Public Health* **2009**, *6* (4), 1418-42.
25. Cao, F.; Sturchio, N. C.; Ollivier, P.; Devau, N.; Heraty, L. J.; Jaunat, J., Sources and behavior of perchlorate in a shallow Chalk aquifer under military (World War I) and agricultural influences. *Journal of Hazardous Materials* **2020**, *398*, 123072.
26. Constantinou, P.; Louca-Christodoulou, D.; Agapiou, A., LC-ESI-MS/MS determination of oxyhalides (chlorate, perchlorate and bromate) in food and water samples, and chlorate on household water treatment devices along with perchlorate in plants. *Chemosphere* **2019**, *235*, 757-766.
27. Ting, D.; Steinmaus, C., Perchlorate: Human Toxicity. In *Encyclopedia of Environmental Health*, Nriagu, J. O., Ed. Elsevier: Burlington, 2011; pp 364-370.
28. Sijimol, M. R.; Mohan, M., Environmental impacts of perchlorate with special reference to fireworks—a review. *Environmental Monitoring and Assessment* **2014**, *186* (11), 7203-7210.
29. Esmeray, E.; Aydin, M., *PERCHLORATE (ClO₄⁻) SOURCES IN DRINKING WATER AND TREATMENT METHODS*. 2010.
30. Munster, J.; Hanson, G., Perchlorate and ion chemistry of road runoff. *Environmental Chemistry* **2009**, *6*.
31. Murray, C. W.; Bolger, P. M., Environmental Contaminants: Perchlorate. In *Encyclopedia of Food Safety*, Motarjemi, Y., Ed. Academic Press: Waltham, 2014; pp 337-341.
32. Morrison, R. D.; Vavricka, E. A.; Duncan, P. B., 9 - Perchlorate. In *Environmental*

Forensics, Morrison, R. D.; Murphy, B. L., Eds. Academic Press: Burlington, 1964; pp 167-185.

33. Kosaka, K.; Asami, M.; Kunikane, S., Perchlorate: Origin and Occurrence in Drinking Water☆. In *Reference Module in Earth Systems and Environmental Sciences*, Elsevier: 2013.

34. Leung, A. M.; Pearce, E. N.; Braverman, L. E., Perchlorate, iodine and the thyroid. *Best Pract Res Clin Endocrinol Metab* **2010**, *24* (1), 133-41.

35. Lisco, G.; De Tullio, A.; Giagulli, V. A.; De Pergola, G.; Triggiani, V., Interference on Iodine Uptake and Human Thyroid Function by Perchlorate-Contaminated Water and Food. *Nutrients* **2020**, *12* (6).

36. Strawson, J.; Zhao, Q.; Dourson, M., Reference dose for perchlorate based on thyroid hormone change in pregnant women as the critical effect. *Regulatory Toxicology and Pharmacology* **2004**, *39* (1), 44-65.

37. Lamb, J. D.; Simpson, D.; Jensen, B. D.; Gardner, J. S.; Peterson, Q. P., Determination of perchlorate in drinking water by ion chromatography using macrocycle-based concentration and separation methods. *J Chromatogr A* **2006**, *1118* (1), 100-5.

38. Shi, Y.; Zhang, P.; Cai, Y.; Mou, S., Improved ion chromatography method for determination of trace level perchlorate in environmental water. *Frontiers of Chemistry in China* **2008**, *3*, 203-208.

39. Kim, Y.; Amemiya, S., Stripping Analysis of Nanomolar Perchlorate in Drinking Water with a Voltammetric Ion-Selective Electrode Based on Thin-Layer Liquid Membrane. *Analytical Chemistry* **2008**, *80* (15), 6056-6065.

40. Almeer, S. H.; Zogby, I. A.; Hassan, S. S., Novel miniaturized sensors for potentiometric batch and flow-injection analysis (FIA) of perchlorate in fireworks and propellants. *Talanta* **2014**, *129*, 191-7.

41. Braik, M.; Dridi, C.; Ali, A.; Abbas, M. N.; Ben Ali, M.; Errachid, A., Development of a perchlorate sensor based on Co-phthalocyanine derivative by impedance spectroscopy measurements. *Organic Electronics* **2015**, *16*, 77-86.

42. Memon, A. A.; Solangi, A. R.; Memon, S.; Bhatti, A. A.; Bhatti, A. A., Highly

Selective Determination of Perchlorate by a Calix[4]arene based Polymeric Membrane Electrode. *Polycyclic Aromatic Compounds* **2016**, *36* (2), 106-119.

43. Ertürün, H. E. K.; Özel, A. D.; Ayanoglu, M. N.; Şahin, Ö.; Yılmaz, M., A calix[4]arene derivative-doped perchlorate-selective membrane electrodes with/without multi-walled carbon nanotubes. *Ionics* **2017**, *23* (4), 917-927.

44. Hassan, S. S. M.; Galal Eldin, A.; Amr, A. E.-G. E.; Al-Omar, M. A.; Kamel, A. H. Single-Walled Carbon Nanotubes (SWCNTs) as Solid-Contact in All-Solid-State Perchlorate ISEs: Applications to Fireworks and Propellants Analysis *Sensors* [Online], 2019.

45. Kuang, B.; Mahmood, H.; Quraishi, Z.; Hoogmoed, W.; Mouazen, A.; Van Henten, E. J., Sensing Soil Properties in the Laboratory, In Situ, and On-Line. *Advances in Agronomy* **2012**, *114*, 155-224.

46. Amemiya, S., Potentiometric Ion-Selective Electrodes. In *Handbook of Electrochemistry*, Zoski, C. G., Ed. Elsevier: Amsterdam, 2007; pp 261-294.

47. Dana, V.; Plesu, N.; Fagadar-Cosma, G.; Lascu, A.; Petric, M.; Crisan, M.; belean, A.; Fagadar-Cosma, E., Potentiometric Sensors for Iodide and Bromide Based on Pt(II)-Porphyrin. *Sensors* **2018**, *18*.

48. Bakker, E.; Bühlmann, P.; Pretsch, E., Carrier-Based Ion-Selective Electrodes and Bulk Optodes. 1. General Characteristics. *Chemical Reviews* **1997**, *97* (8), 3083-3132.

49. Sánchez-Pedreño, C.; Ortuño, J. n. A.; Hernández, J., Perchlorate-selective polymeric membrane electrode based on a gold(I) complex: application to water and urine analysis. *Analytica Chimica Acta* **2000**, *415* (1), 159-164.

50. Shamsipur, M.; Sadeghi, S.; Naeimi, H.; Sharghi, H., Iodide ion-selective PVC membrane electrode based on a recently synthesized salen-Mn(II) complex. *Polish Journal of Chemistry* **2000**, *74*, 231-238.

51. Shamsipur, M.; Rouhani, S.; Mohajeri, A.; Ganjali, M.; Rashidi, P., A bromide ion-selective polymeric membrane electrode based on a benzo-derivative xanthenium bromide salt. *Analytica Chimica Acta* **2000**, *418*, 197-203.

52. Poursaberi, T.; Salavati-Niasari, M.; Khodabakhsh, S.; Hajiaghababaei, L.; Shamsipur, M.; Yousefi, M.; Rouhani, S.; Ganjali, M., A selective membrane electrode for thiocyanate ion based on a copper-1,8-dimethyl-1,3,6,8,10,13-azacyclotetradecane

complex as ionophore. *Analytical Letters - ANAL LETT* **2001**, *34*, 2621-2632.

53. Itterheimová, P.; Bobacka, J.; Šindelář, V.; Lubal, P., Perchlorate Solid-Contact Ion-Selective Electrode Based on Dodecabenzylbambus[6]uril. *Chemosensors* **2022**, *10* (3), 115.

54. Chen, L. D.; Zou, X. U.; Bühlmann, P., Cyanide-Selective Electrode Based on Zn(II) Tetraphenylporphyrin as Ionophore. *Analytical Chemistry* **2012**, *84* (21), 9192-9198.

55. Lisak, G.; Tamaki, T.; Ogawa, T., Dualism of Sensitivity and Selectivity of Porphyrin Dimers in Electroanalysis. *Analytical Chemistry* **2017**, *89* (7), 3943-3951.

56. Mitchell-Koch, J. T.; Pietrzak, M.; Malinowska, E.; Meyerhoff, M. E., Aluminum(III) Porphyrins as Ionophores for Fluoride Selective Polymeric Membrane Electrodes. *Electroanalysis* **2006**, *18* (6), 551-557.

57. Shamsipur, M.; Soleymanpour, A.; Akhond, M.; Sharghi, H.; Hasaninejad, A. R., Perchlorate selective membrane electrodes based on a phosphorus(V)-tetraphenylporphyrin complex. *Sensors and Actuators B: Chemical* **2003**, *89* (1), 9-14.

58. Han, H.; Kim, H.-J.; Jung, D.-H.; Cho, W., Real-time Nutrient Monitoring of Hydroponic Solutions Using an Ion-selective Electrode-based Embedded System. *Protected horticulture and Plant Factory* **2020**, *29*, 141-152.

59. Szigeti, Z.; Malon, A.; Vigassy, T.; Csokai, V.; Grün, A.; Wygladacz, K.; Ye, N.; Xu, C.; Chebny, V. J.; Bitter, I.; Rathore, R.; Bakker, E.; Pretsch, E., Novel potentiometric and optical silver ion-selective sensors with subnanomolar detection limits. *Anal Chim Acta* **2006**, *572* (1), 1-10.



จุฬาลงกรณ์มหาวิทยาลัย
CHULALONGKORN UNIVERSITY

VITA

NAME Kawisara Longsakpreecha

DATE OF BIRTH 16 April 1998

PLACE OF BIRTH Phrae

INSTITUTIONS ATTENDED Chulalongkorn University

HOME ADDRESS 69/1 Moo 2 Subdistrict Bangnga District Tha Wung
Province Lopburi Postal code 15150

PUBLICATION Pure Applied Chemistry International Conference



จุฬาลงกรณ์มหาวิทยาลัย
CHULALONGKORN UNIVERSITY